We are IntechOpen, the world's leading publisher of Open Access books Built by scientists, for scientists

6,900
Open access books available

185,000
International authors and editors

200M
Downloads

Our authors are among the

154
Countries delivered to

TOP 1%
most cited scientists

12.2%
Contributors from top 500 universities



WEB OF SCIENCE™

Selection of our books indexed in the Book Citation Index in Web of Science™ Core Collection (BKCI)

Interested in publishing with us?
Contact book.department@intechopen.com

Numbers displayed above are based on latest data collected.
For more information visit www.intechopen.com



Chapter 10

Bronchology – A Well Branched Tree

Mihai Olteanu, Costin Teodor Streba,
Bogdan Oprea, Raluca Marinas, Mimi Floarea Nitu,
Emilia Crisan and Tudorel Ciurea

Additional information is available at the end of the chapter

http://dx.doi.org/10.5772/52748

1. Introduction

1.1. Lung cancer – Stadialization

Lung cancer is responsible for 1.3 million deaths worldwide annually, and it is the most common cause of cancer-related death in men and the second most common in women. Lung cancer staging is the assessment of the degree to which a lung cancer has spread from its original source. As with most cancers, for lung cancer staging is of paramount importance for the treatment planning process and prognosis. Two primary methods of lung cancer staging are available: clinical staging and pathologic staging. In clinical staging, information is provided by noninvasive or minimally invasive techniques, such as physical examination, radiologic examination, endoscopic ultrasound, bronchoscopy, mediastinoscopy, and thoracoscopy. In pathologic staging, information obtained from clinical staging is combined with findings from both the invasive surgical procedure and the pathologic evaluation of excised tissue. Clinical staging is important and can help to determine the next appropriate step in therapy, such as the decision to proceed with pathologic staging, which remains the reference standard because the overall level of agreement between the two systems only ranges from 35% to 55% [1].

Definition of the stage is an essential part of the approach to patients with lung cancer, and it has led to the development of a universally accepted stage classification systems for most tumors. The Union Internationale Contre le Cancer (UICC) and the American Joint Committee on Cancer (AJCC) periodically define, review, and refine the stage classification systems. Nearly half of all patients with lung cancer have mediastinal disease at diagnosis, and this implies metastases to ipsilateral or subcarinal nodes (N2) that are classified as stage IIIA dis-

INTECH
open science | open minds

© 2013 Olteanu et al.; licensee InTech. This is an open access article distributed under the terms of the Creative Commons Attribution License (http://creativecommons.org/licenses/by/3.0), which permits unrestricted use, distribution, and reproduction in any medium, provided the original work is properly cited.

ease. Management of stage IIIA disease is more controversial, but many centers treat it with radiation and chemotherapy, with surgery performed under investigational protocols. Direct mediastinal invasion (T4) or metastasis to contralateral mediastinal nodes (N3) is classified as stage IIIB disease. The 5-year survival rate in this case is at best 5%, and patients are generally offered treatment with chemoradiotherapy without surgery.

The previous tumor, node, and metastasis (TNM) classification, the sixth edition of the TNM Classification of Malignant Tumors, was published in 2002. The last revision of the staging system for lung cancer has been presented by Dr. Clifton Mountain in 1997 [2], after his proposal had been adopted in 1973 by the AJCC in the same year and by the UICC in 1974, and this revision remained unaltered on the 2002 manual [3]. The 1973 original system was based on a database of 2,155 patients from the MD Anderson Cancer Center in Houston, TX. Subsequent revisions of the TNM staging system continued to be based on this database, which grew to include 5,319 cases at the time the lung cancer staging system was revised in 1997 and it was also validated by Dr. Naruke from Japan in 2001. Mountain's revision was based on a relatively small population of patients who underwent surgical treatment in a single geographic area, and no validation was presented to justify the individual descriptors [4]. In order to overcome the limitations of the sixth TNM classification, the International Association for the Study of Lung Cancer (IASLC) launched the Lung Cancer Staging Project in 1996, and in 1998 created an International Staging Committee (ISC) of multidisciplinary members to conduct revisions [5]. Changes to the sixth edition were proposed by the IASLC based on an international collection and review of 100,869 patients from 46 sources of 20 countries. Data were drawn from lung cancer cases treated by all modalities between 1990 and 2000. After exclusion of ineligible cases, 81,015 patients (67,725 NSCLC and 13,290 SCLC) remained for investigation [6]. Proposals for revision were submitted to the AJCC and UICC for consideration in the new edition of the staging manual, the 7th, and both accepted the recommendations. In the last months of 2009, the Seventh Edition of the TNM Classification of Malignant Tumors was published, with a new lung cancer staging system. The new edition took effect on January 1, 2010 [7].

The changes recommended by the IASLC for the 7th edition of TNM classification for lung cancer were based on differences in survival [8], and the results of the data analysis were internally and externally validated [9]. These changes include new T and M definitions and consequent new stage groupings, a new lymph node map, a novel definition on pleural invasion, as well as recommendations to apply the TNM system to broncho-pulmonary carcinoid tumors and SCLC.

The success story of EBUS-TBNA starts in 2003 with a publication in Thorax by Mark Krasnik and Peter Vilmann from Gentofte University Hospital, Denmark [10]. This article gave the first description of the principle of EBUS-TBNA. In the same journal, in 2006, the same group, together with a group from the Thoraxklinik in Heidelberg and Harvad Medical School's Beth Israel Deaconess MC, published their study on 502 patients that showed that EBUS-TBNA resulted in 93% diagnostic yield, a sensitivity of 94%, specificity of 100% and accuracy 94%, with PPV at 100% and NPV at 11% [11]. In 2006, an international EBUS-TBNA focus group was formed by Felix J.F. Herth (Copenhagen), Kazuhiro Yasufu-

ku (Chiba), Robert Rintoul (Cambridge) and Armin Ernst (Boston) that published in the Journal of Bronchology a description of how to do an EBUS-TBNA thus offering a detailed description of local lymph node position and orientation within the mediastinum [12]. EBUS-TBNA has been studied and compared also in relation with existing modalities like EUS –FNA (by Vilmann et al. in 2005 on 33 pts. and by Herth et al. in 2005 on 160 pts.), PET-CT (by Yasufuku et al. in 2006 on 102 pts.), classical TBNA and EUS-FNA (by Wallace et al. in 2008 on 138 pts.).

EBUS-TBNA was proven in 2007 by Wong and Yasufuku et al. on 65 patients to be a safe method allowing a high yield also for the diagnosis of sarcoidosis [13].

It soon became widely accepted that EBUS-TBNA is a reliable diagnostic tool for enlarged lymph nodes in patients with NSCLC and that lymph nodes below the one centimeter range could also be sampled. This led to a study with 100 patients published in 2006 in European Respiratory Journal [14] that showed that every sixth patient with no evidence of mediastinal disease on CT was diagnosed positive using EBUS-TBNA. Thus, EBUS-TBNA showed potential to avoid unnecessary exploratory thoracoscopies. Following the same idea, in 2008 Hwangbo et al. showed that in cases with both CT- and PET-negative and –positive scans, EBUS-TBNA is an excellent tool for detecting mediastinal metastasis, thereby confirming that EBUS-TBNA is an effective invasive method following CT and PET scanning [15].

In the same year, Armin Ernst et al. showed in Journal of Thoracic Oncology on 66 patients that EBUS-TBNA can have a superior yield compared to cervical mediastinoscopy, which intuitively suggested that mediastinoscopy is not necessarily of additional diagnostic benefit in evaluating negative EBUS-TBNA staged lymph nodes [16]. However, mediastinoscopy has an important role especially in operable patients with non-enlarged lymph nodes for assessing local mediastinal invasion and the exclusion of metastatic disease.

Herth et al. evaluated EBUS-TBNA for re-staging in 124 patients with tissue-proven IIIA-N2 disease after induction chemotherapy (Journal of Clinical Oncology 2008) and concluded that EBUS-TBNA is a valuable and practical tool for re-staging with a sensitivity of 76%, specificity of 100%, PPV of 100%, NPV of 20% and diagnostic accuracy of 77% [17]. These results imply that a negative EBUS-TBNA for re-staging should be surgically re-staged.

In 2006, the compatibility between EBUS-TBNA and the Aloka Prosound alpha5 ultrasound processor made additional Doppler modes available, and this led to a consecutive study by Herth et al. on 89 patients that described changes in flow resistance parameters (resistance index by Pourcelot) in malignant lymph nodes [18].

Yasufuku et al. from Chiba University have shown great dedication to evaluating the benefits of EBUS-TBNA samples for immunohistochemical analysis and reported encouraging results with cell cycle-related proteins in chemotherapy patients in Thorax 2008, and a year earlier in Chest the same group showed that epidermal growth factor receptor (EGFR) mutation can be easily detected in metastatic lymph node samples for EBUS-TBNA and so the samples gained by EBUS-TBNA allowed genetic evaluations of tumour cells from lymph nodes [19, 20].

In 2009 Tournoy et al. provided a detailed analysis of endosonographic landmarks (where available), describing the anatomic borders of the lymph node stations as defined in the 7th edition of the IASLC's TNM-staging nomenclature, which is relevant for correctly staging patients with lung cancer [21].

Building on the strong results of combined EUS-FNA and EBUS-TBNA procedures – a study published by Vilman et al. in 2005 had already indicated their complementary nature – Annema et al. challenged in 2010 the pre-dominant surgical staging algorithm by comparing the combined EBUS-TBNA and EUS-TNA with surgical staging alone [22] and showed that combining endosonographic and surgical staging resulted in greater sensitivity for mediastinal nodal metastases and fewer unnecessary thoracotomies. These results indicated that the combination of both procedures may be able to replace surgical stages as the primary staging method for patients with lung cancer.

Instead of using different scopes for EBUS-TBNA and EUS-TNA, two separate studies published in Chest in 2010 by Hwangbo et al. and Herth et al. [23] used only one bronchoscope for both procedures, starting via the trachea and continuing via the oesophageal route. They came to the conclusion that EBUS-TBNA and EUS-TNA are complementary methods and showed that both procedures can be performed with a single EBUS echoendoscope in one sitting by one operator. A further study in 2011, "Nonsurgical staging of the mediastinum: EBUS and EUS" conducted by Herth, stated that the combination of both procedures achieves a complete and accurate mediastinal staging. Therefore it can be expected that the implementation of combined EBUS-TBNA and EUS-FNA will reduce the need for surgical staging of lung cancer significantly [24].

The summary of scientific studies on EBUS-TBNA provided about clearly shows the procedure's power in helping to improve mediastinal staging of lung cancer during the past 10 years. The technological development of less invasive staging and sampling devices continues endoscopists using endosonography, we can expect further exciting developments in clinical practice in the years to come.

Endobronchial ultrasound with real-time-guided transbronchial fine-needle aspiration (EBUS-TBNA) is a minimally invasive outpatient procedure by which mediastinal [25] and hilar lymph nodes [26] as well as centrally located primary lung lesions [27] can be visualised and sampled under ultrasound guidance. In a systematic review, EBUS-TBNA has shown a pooled sensitivity of 93% in the staging of non-small-cell lung cancer. In a direct comparison with surgical staging, EBUS-TBNA even showed to be superior [28]. Therefore, EBUS-TBNA has been adopted in the most recent lung cancer staging guidelines as a minimally invasive alternative to surgical staging [29]

EBUS-TBNA is an accurate, minimally invasive and safe staging procedure and can be considered the procedure of choice for patients with extrathoracic malignancies in whom hilar or mediastinal lesions are observed. In patients with (concurrent or previously treated) extrathoracic malignancy, EBUS-TBNA has a sensitivity of 85% to demonstrate metastatic spread. Implementation of EBUS-TBNA in these patients obviates invasive surgical diagnostic procedures in 61%. [30, 31]

http://dx.doi.org/10.5772/52748

The development and introduction of the new convex probe endobronchial ultrasound (CP-EBUS) that performs endobronchial ultrasound-guided transbronchial needle aspiration has changed the practice of bronchoscopic biopsy of the mediastinum in respiratory diseases. In particular, the role of EBUS-TBNA in the diagnosis and mediastinal lymph node staging of lung cancer, the leading cause of death from malignant disease worldwide [32], is becoming an interest to pulmonologists as well as thoracic surgeons. The newest CP-EBUS now being used in clinical practice is a hybrid bronchofibervideoscope which features a unique optical system that exploits both video and fiber-optic technologies (BFUC160F- OL8, Olympus, Tokyo, Japan). This CP-EBUS is a linear curved array transducer that scans parallel to the insertion direction of the bronchoscope. Images can be obtained by directly contacting the probe or by attaching a balloon on the tip and inflating with saline (Figure 1). The outer diameter of the insertion tube of the CP-EBUS is 6.2 mm, and that of the tip is 6.9 mm. The angle of view is 80º and the direction of view is 35º forward oblique [33].

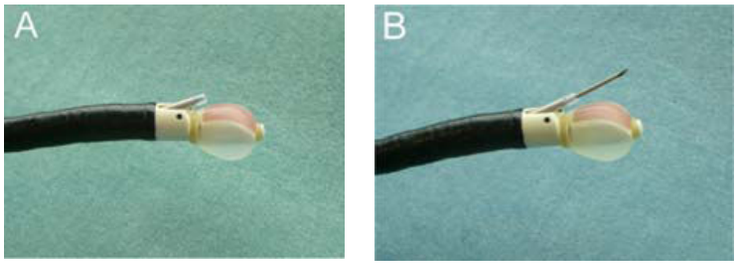


Figure 1. Tip of the new convex probe endobronchial ultrasound (CP-EBUS, BF-UC160FOL8, Olympus, Tokyo, Japan). The outer diameter of the insertion tube of the flexible bronchoscope is 6.2 mm. CP-EBUS has a linear curved array ultrasonic transducer of 7.5 MHz. The balloon attached to the tip of the bronchoscope is inflated with normal saline (A). The dedicated TBNA needle is inserted through the working channel (B) [33].

The built-in CCD in the control section allows sharp images similar to those of regular videoscopes and allows a slimmer insertion tube of 6.2 mm. The ultrasound images can be frozen and the size of lesions can be measured in two dimensions by the placement of cursors. It is also equipped with the Color Power Doppler mode. The display range covers 2–24 cm (Figure 2).



Figure 2. The convex probe endobronchial ultrasound (CP-EBUS, BF-UC160F-OL8, Olympus, Tokyo, Japan) and The dedicated ultrasound processor (EU-C60/EU-C2000, Olympus, Tokyo, Japan) [33].

The dedicated 22-gauge needle is used for EBUS-TBNA (Figure 3). The needle is a single use aspiration needle with echogenic dimpled tip design to improve visibility on ultrasound images. This needle has various adjuster knobs which work as a safety device to prevent damage to the channel. The maximum extruding stroke is 40 mm and to prevent excessive protrusion, a safety mechanism stops the needle at the stroke of 20 mm. The needle is attached onto the working channel of the bronchoscope which allows the operator to actually perform EBUS-TBNA. The needle is also equipped with an internal sheath which is withdrawn after passing the bronchial wall, avoiding contamination during TBNA. This internal sheath is also used to clear out the tip of the needle after passing the bronchial wall. The use of this sheath has significantly increased the yield of EBUS-TBNA. The exit of the needle is at 20° with respect to the outer covering of the insertion tube. The needle can be visualized through the optics and on the ultrasound image [33].

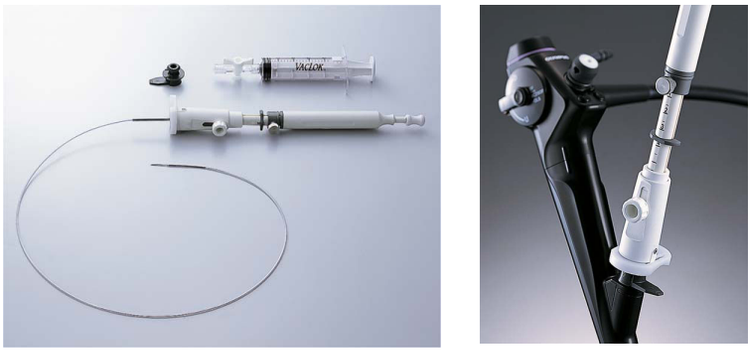


Figure 3. A Dedicated 22-gauge needle (NA-201SX-4022, Olympus, Tokyo, Japan) and the Vaclok syringe used to create negative pressure. B The needle attached to the working channel of the EBUS-TBNA bronchoscope. The maximum extruding stroke is 40 mm and to prevent excessive protrusion, a safety mechanism stops the needle at the stroke of 20 mm [33].

Mediastinal staging can be divided into noninvasive staging (imaging) and invasive (sampling) staging. Computed tomography (CT), magnetic resonance imaging (MRI), positron emission tomography (PET) and PET-CT are used for noninvasive imaging [34]. Other imaging modalities include the use of transesophageal ultrasonography (EUS) and endobronchial ultrasound (EBUS) using a radial probe for detecting even small mediastinal lymph nodes [35-36]. Mediastinoscopy is still the gold standard for mediastinal lymph node staging [37]. However, it requires general anesthesia and complications cannot be ignored.

1.2. Changes to T descriptors [38-39]

Rami-Porta R et al. evaluated in 2007 for the 7th Edition of the TNM Classification of Malignant Tumors only patients without metastasis and, although there was information about different aspects of the T component, they only could analyze in detail tumor size, existence of accompanying nodules and pleural dissemination.

The prognostic value of the tumor size was studied in patients with completely resected pathological T1 and T2 N0 M0 tumors who had not received adjuvant therapy. The statisti-

http://dx.doi.org/10.5772/52748

cal calculations determined three cut-points at 2, 5 and 7cm, which, in addition to the 3cm, the border between T1 and T2, gave rise to 5 groups of tumors with significantly worse survival with larger tumor diameters. The groups and their 5-year survival rates were: T1≤2cm, 77%; T1>2cm and ≤3cm, 71%; T2>3cm and ≤5cm, 58%; T2>5cm and ≤7cm, 49%, and T2>7cm, 35%. This prognostic gradation was maintained when less selective patient populations were evaluated: clinical staging, incomplete resection and different lymph node affectation. With such arguments, it was decided to subdivide the T1 tumors into T1a (≤2cm) and T1b (>2cm and ≤3cm), and T2 tumors into T2a (>3cm and ≤5cm) and T2b (>5cm and ≤7cm). Likewise, the 5-year survival was compared between patients with T2>7cm tumors and T3 tumors. Similar results were found in the different populations, except in the N0 cases with complete resection, in which it was verified that the survival was even higher in the T3 (41%) than in the T2>7cm (35%), therefore it was decided to reclassify the latter as T3. When they analyzed the tumors that, with pathological staging, presented additional nodules, it was observed that: (a) the 5-year survival of the T3 (31%) was similar to the T4 classified as such due to the existence of an additional nodule or nodules in the same lobe as the primary tumor (28%); (b) the T4 due to other factors had the same survival as those classified as M1 due to an additional nodule(s) in a different homolateral lobe than the primary tumor (22%); and (c) the T4 due to pleural dissemination had a clearly worse prognosis (11% 5-year survival). For the new classification, it was therefore recommended to consider as T3 those tumors with additional nodule(s) in the same lobe as the primary tumor, to consider as T4 those tumors with additional nodule(s) in a homolateral lobe other than that of the primary tumor, and to include in the M category those tumors with pleural dissemination (Table 1).

T descriptor		6th ed.	7th ed.
T size	Tumors = 2 cm	T1	T1a
	Tumors > 2 cm and = 3 cm		T1b
	Tumors > 3cm and = 5cm	T2	T2a
	Tumors > 5 cm and = 7 cm		T2b
	Tumors > 7 cm		T3
Separate nodule(s) in the primary lobe.		T4	T3
Separate nodule(s) in a different ipsilateral lobe.		M1	T4
Malignant pericardial effusion.		T4	M1a
Pleural dissemination.		T4	M1a

Table 1. T descriptor changes: comparison between 6th and 7th edition of the TNM Classification of Malignant Tumors [38]

1. *Tumor size cut points at 2, 3, 5, and 7 cm:*

• T1 subclassified:

- T1a: tumors = 2 cm

- T1b: tumors: > 2 cm and = 3 cm

• T2 subclassified:

- T2a: > 3cm and = 5cm

- T2b: > 5 cm and = 7 cm

• T2 reclassified:

- T2 > 7 cm became T3.

2. *Multicentric tumors of similar histology:*

- Separate nodule(s) in the primary lobe: became T3 from T4.

- Separate nodule(s) in a different ipsilateral lobe: became T4 from M1.

3. *T4 descriptors:*

- Pleural dissemination (pleural nodules or malignant effusion): became M1a from T4.

- Malignant pericardial effusion: became M1a from T4.

In the *AJCC Cancer Staging Manual* and *UICC TNM Classification of Malignant Tumors* the T factor is divided into four descriptors (T1-4) depending on size, site, number, and local extent of the primary tumor: the size and non-size based descriptors [40].

1.2.1. Size-based T descriptors

The value of tumor size in NSCLC prognosis is supported by large clinical evidence [41-45]. The tumor size threshold of 3 cm was set-up on the 2nd edition of the TNM classification of malignant tumors in 1974.[46], and despite the advances in surgical procedures, adjuvant treatment, and mostly in imaging technology, this measure remained unchanged for 35 years. The 7th edition of the TNM for lung cancer confers more importance to the size-based T descriptors and divides them as seen earlier. These modifications have been validated by recent studies that showed better survival stratification and prognosis estimation with the new T definitions [47-49].

Table 2a describes lower survival rates as the T factor increases [50-51].; survival rates are improved with the new system due to reclassification (up- and down-staging) of patients when compared to series reporting survival rates with the previous TNM, showed in Table 2b [52-53].

http://dx.doi.org/10.5772/52748

T component	5-year survival (%)	
	Kameyama et al [25]	Li et al [24]
T1a	82.6	75.49
T1b	73.3	74.58
T2a	63.5	60.87
T2b	50.1	55.63
T3	40.6	46.15
T4	34.6	NS

T component	5-year survival (%)	
	Mountain CF [26]	Naruke et al. [27]
T1	67	68.9
T2	57	42.5
T3	38	31.9
T4	7 (cT)	18.9

Table 2. a. Five year survival by pT classification with the 7th edition. **b.** Five year survival by pT classification with the 6th edition [40].

1.2.2. Non–size-based T descriptors

1.2.2.1. Multiple nodules

The existence of multiple primary cancers (MPC) was initially reported by Warren and Gates in 1932 [54], but in spite of these past 80 years, to date accurate diagnosis of MPC is not yet clearly established due to a lack of consensus on definition and diagnostic criteria [55]

In 1975, Martini and Melamed were the first to propose clinical and histopathologic criteria for the differential diagnosis of second lung cancers [56]. MPLCs are defined synchronous, if detected simultaneously, or metachronous, if tumors are separated in time [57-58]. Synchronous nodules may represent a MPLC (second primary), a metastasis, or an extension from the primary (satellite nodule) [59] (Table 3).

Deslauriers et al. described in 1989 intrapulmonary nodular metastasis in patients with NSCLC as satellite nodules, and the 5- year survival rates for these patients with satellite nodules were 21.6% compared to 44% for patients without satellite nodules. They concluded that patients with satellite nodules should be classified as stage IIIA [60].

Type		Definition
Satellite nodule		Same histology And same lobe as primary cancer And no systemic metastasis
MPLCs	Same histology, anatomically separated	Tumors in different lobes And no N2-3 involvement And no systemic metastasis
	Same histology, temporally separated	=4-yr interval between tumors And no systemic metastasis from either tumor
	Different histology	Or different molecular genetic features Or arising separately from foci of CIS
Metastasis	Same histology	With multiple systemic metastasis
	Same histology, in different lobes	And presence of N2-3 involvement Or < 2-yr interval

Table 3. Definitions of second primary, satellite nodules and metastasis [61-62].

The concept of satellite nodules was not considered in NSCLC staging system until 1992 by the AJCC and in 1993 by the UICC [63-64].

Prior to this, all nodules were classified as M1.

The T4 descriptor includes diverse tumors with different evolution and prognosis:

- invasion of the mediastinum, heart, great vessels, trachea, esophagus, vertebral body, and carina;
- tumor with a malignant pleural or pericardial effusion, or with satellite tumor nodule(s) within the ipsilateral primary-tumor lobe of the lung.

The IASLC lung cancer staging project committee has acknowledged the multiple reports showing better survival for primary tumors with satellite nodules than other T4 tumors and this is the reason why they downstaged them accordingly [38,65].

Later studies found that the new T descriptor for satellite nodules proposed by the IASLC reflects better the outcomes of that group of patients, which showed superior survival rates, and now these patients are to be considered for surgery [66-67].

1.2.2.2. Pleural dissemination and pericardial effusion

According to the TNM staging manual, pleural dissemination is defined as the presence of ipsilateral malignant pleural effusion (MPE) or pleural nodules [68]. Pleural nodules are defined as pleural tumor foci separated from direct pleural invasion by the primary tumor, classified as T4 [69]. These pleural tumors must be differentiated from direct tumor invasion to the visceral (T2) or parietal pleura (T3) (Table 4).

PL category	Definition	T status	
PL0	Tumor within the subpleural parenchyma or, invading superficially into the pleural connective tissue below the elastic layer.	PL0 is not a T descriptor and the T component should be assigned on other features.	
PL1	Tumor invades beyond the elastic layer.	**pT2**	**Indicates VPI**
PL2	Tumor invades to visceral pleural surface.		
PL3	Tumor invades the parietal pleura.	pT3	

Table 4. Classification of visceral pleural invasion (VPI): Proposed modification of Hammar Classification [70]

Introduction of a new accurate definition of visceral pleural invasion (VPI); VPI is a pT2 descriptor (Table 4). The abbreviation PL is used instead of P which is also used for designation of pTNM in distinction from cTNM. The IASLC also recommends the use of elastic stains to distinguish between PL0 and PL1 when hematoxylin and eosin (H&E) sections are not helpful [71].

In TNM staging, either pleural fluid cytology or clinical judgment are valid to establish the diagnosis of a MPE and consider it as a T4 factor [72], in the absence of relevant conventional or guided pleural biopsy. Malignant pericardial effusions are classified according to the same rules. Pleural dissemination and pericardial effusion are T4 descriptors, grouped into stage IIIB in absence of distant metastasis. The MPE is considered to be a sign of advanced disease, and almost every cancer can involve the pleura [73-74]. However, most MPE's are due to NSCLC's and encompass the worst prognosis [75-77], even worse than in the presence of satellite nodules or mediastinal invasion; only a few patients survive beyond 12 months, regardless of treatment modality, surgery or not, according to studies by Osaki et al., Sugiura et al., Mott et al. and Kameyama et al. [78-81]

Ipsilateral MPE is a locally advanced disease that precludes surgical treatment in lung cancer [82-83]. Unlike other malignant effusions, those caused by NSCLC have low sensitivity to chemo- and radiotherapy [84-86]; therefore these patients are candidates for palliative therapy. In a similar way, NSCLC is the most frequent cause of malignant pericardial effusion, which has a grim prognosis too [87-89].

The IASLC reclassified pleural dissemination from T4 to M1a based on the magnitude of evidence demonstrating that postoperative survival rates of patients with stage IIIB due to MPE are no different from those with stage IV disease and significantly lower than in patients with no pleural effusion and even with non-malignant pleural effusion [90-95].

Status at thoracotomy	5-year survival (%)
No pleural effusion	45.4
Non-MPE	42.5
MPE	15.9
Pathologic stage IV	11.2

Table 5. Postoperative survival rates of NSCLC with malignant pleural effusion (MPE): no significant difference with stage IV disease. (Data from Naruke et al [96])

1.3. Changes to N descriptors [97-98]

The accurate assessment of lymph node involvement is an important part of the management of lung cancer. Lymph node "maps" have been used to describe the location of nodal metastases. However, there are discrepancies in nomenclature among maps used by Asian and Western countries. The IASLC proposed a new lymph node map that reduces these differences among currently used maps, and provides precise anatomic definitions for all lymph node stations. It has also been proposed a new method of grouping lymph node stations together into "zones" for the sake of future survival analyses [99].

Milestones:

1. No changes were made to N descriptors. Analysis from the international database of the IASLC showed that current N descriptors provide good survival stratification, and therefore considered appropriate to maintain them without modifications [100].

2. New International Lymph Node Map: The IASLC has developed a new lymph node chart to resolve disagreements in nomenclature between Naruke's (The Japan Lung Cancer Society) and Mountain-Dresler's maps (American Thoracic Society). Although the nomenclature has changed, the general concept remains the same. Patients without nodal metastatic disease are designated as N0. Patients with N1 disease are defined as having metastatic involvement of lymph nodes in the ipsilateral peripheral or hilar zones. The N2 designation signifies metastatic extension to lymph nodes in the ipsilateral mediastinal (upper, aorticopulmonary, lower) or subcarinal lymph node zones. The N3 nodal designation includes metastatic involvement of any nodes in the supraclavicular lymph node zone or nodes in contralateral mediastinal, hilar–interlobar, or peripheral zone.

3. New classification of lymph nodes by grouping stations into seven "Nodal Zones" for prognostic analysis: supraclavicular, upper, aorticopulmonary, subcarinal, lower, hilar–interlobar, and peripheral (Table 6 and Figure 4); this proposal needs to be validated with prospective studies and it is not yet effective in the new TNM system.

http://dx.doi.org/10.5772/52748

Nodal Zone	Lymph node station
Upper zone	Low cervical, supraclavicular, sternal notch (1R – 1L)
	Upper paratracheal (2R – 2L)
	Prevascular (3a) and retrotracheal (3p)
	Lower paratracheal (4R – 4L)
Aortopulmonary zone	Subaortic (aortopulmonary window - 5)
	Para-aortic (ascending aorta or phrenic nerve - 6)
Subcarinal zone	Subcarinal (7)
Lower zone	Paraesophageal (8)
	Pulmonary ligament (9)
Hilar zone	Hilar (10)
	Interlobar superior (11s) and inferior (11i)
Peripheral zone	Lobar (12)
	Segmental (13)
	Subsegmental (14)

Table 6. Grouping of lymph node stations into "zones".

Survival differences were also calculated on the basis of the number of lymph node zones involved in any single nodal designation. For instance, in pathologically staged patients with any T and M0, those with nodal metastases to a single N1 zone had a median survival of 52 months whereas those with metastatic spread to nodes in multiple N1 zones had a median survival of only 31 months. Similar decreases in survival were also seen in patients with multiple N2 nodal zone involvement (median survival 19 months) compared with those with disease in a single N2 nodal zone (median survival 35 months) [65]. These results showed improved survival in patients with a single N2 zone involved compared with those with multiple N1 zones involved. These findings were validated by an external study [102], and raising the possibility of subdividing the N1 and N2 classifications into N1a (single-zone N1), N1b (multiple-zone N1), N2a (single-zone N2), and N2b (multiple-zone N2).

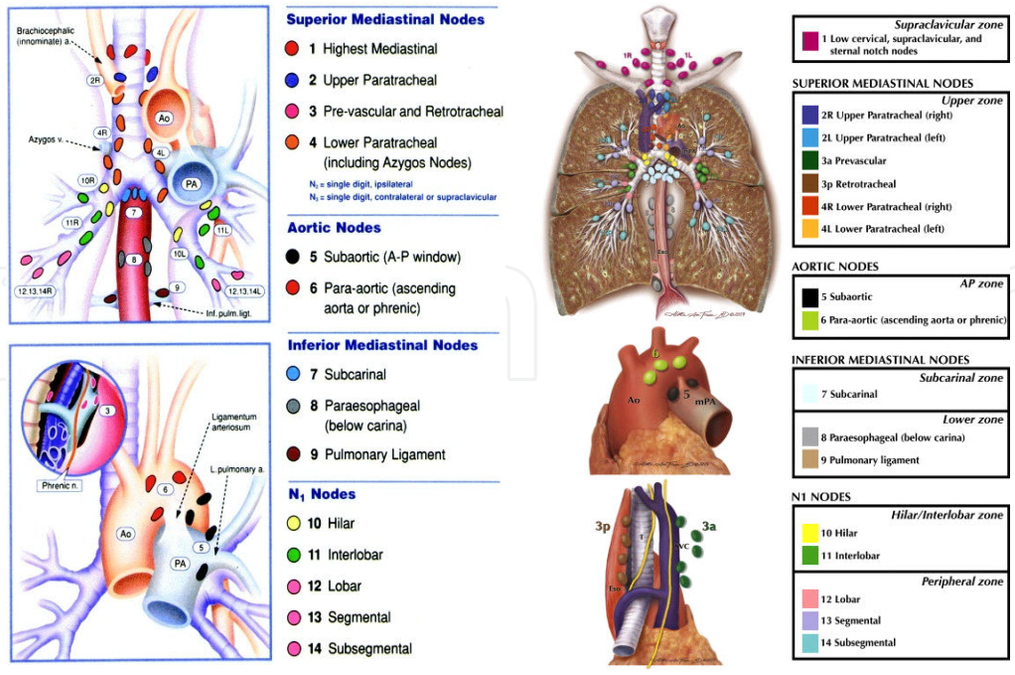


Figure 4. A parallel between previous Mountain-Dresler modified lymph node map originally proposed by the American Thoracic Society and the proposed grouping of lymph node stations into "zones" for the purposes of prognostic analyses from Rusch VW et al. [100].

4. Given the continuous ascension of endoscopic ultrasound techniques such as EBUS (endobronchial ultrasound) and EUS (endocopic ultrasound) guided transbronchial (TBNA) and transesophageal (FNA) fine needle aspiration for the sampling of mediastinal lymph nodes, the borders between lymph node stations have been reconsidered, limiting as much as possible the subjectivism and trying to better standardize and define nodal stations.

As Tournoy et al. showed in this graphic representation, the reach of EUS-FNA and EBUS-TBNA is partly overlapping and partly complementary. EBUS-TBNA follows the large airways, whereas EUS-FNA is excellent for the left, posterior and lower mediastinal and paraoesophageal stations. When both techniques are available, many of the mediastinal and hilar lymph nodes can be reached for fine-needle aspiration. In addition, with EUS-FNA, the left liver lobe, celiac trunk nodes, and the left adrenal gland can be assessed. With EUS, lymph nodes can be identified if they are located in the vicinity of the esophagus. The nodes to be identified with EUS are described in relation to vascular structures (including the aorta, the azygos vein, the left atrium, and the pulmonary artery) and the diaphragm [103-104]. With EBUS, the ultrasound window angle is much smaller, when compared with EUS (50–60 degree angle versus 150– 180 degree angle), which makes the visualization and identification of large vessels or ultrasound landmarks easier with the latter (Figure 5). EUS helps in the identification of structures and landmarks through movements of backward, forward and rotation of the scope. In contrast to EUS, EBUS has the advantage of having a real-time bronchoscopic view into the airways during procedures, which helps with a more accurate identification of the lymph node stations [12].

http://dx.doi.org/10.5772/52748

In general, the lymph nodes are characterized based on EBUS imaging as follows:

a. Size (in short axis): less or more than 1 cm.

b. Shape: oval or round; when the ratio of short vs. long axis of lymph nodes is smaller than 1.5, the lymph node is defined as round; if the ratio is bigger than 1.5, it is oval.

c. Margin: indistinct or distinct; if the majority of the margin (>50%) is clearly visualized with a high echoic border, the lymph nodes are determined as distinct. If the margin is unclear, they are determined as indistinct.

d. Echogenecity: homogeneous or heterogeneous

e. The presence or absence of central hilar structure (CHS); CHS defined as a linear, flat, hyperechoic area in the center of the lymph node.

f. The presence or absence of coagulation necrosis sign (CNS). CNS is a hypoechoic area within the lymph node without blood flow. Typical coagulation necrosis sign represents a low echoic area within the lymph node and that sometimes occupy the majority of the lymph node. The presence of CNS had the highest specificity (92.6%) and the highest hazard ratio (5.6) for prediction of metastatic lymph nodes [106]



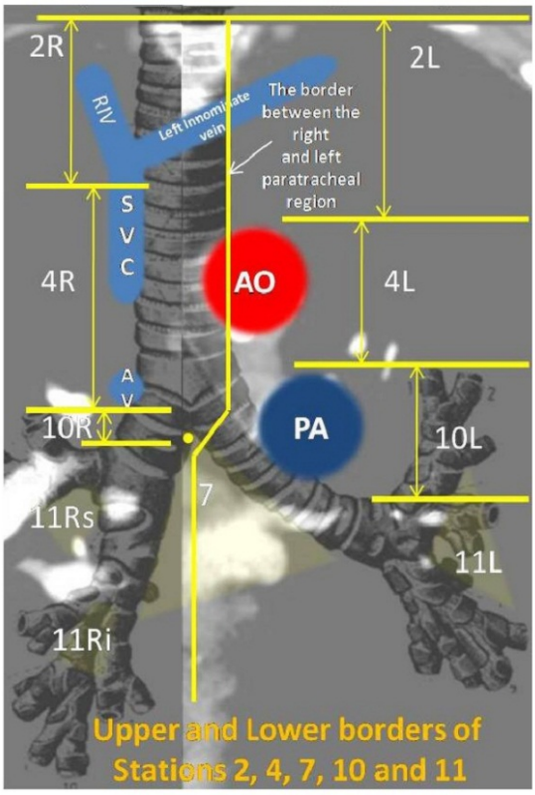
Figure 5. Devices used in endoscopic and endobronchial ultrasound. Endoscopic ultrasound probe (left) and endobronchial ultrasound scope (right) [105].

Since we consider that in the light of the latest TNM classification the knowledge of lymph node stations and their borders is of absolute importance, we will debate about it on a larger scale in this chapter. This, according to our opinion, is going to help especially the EUS-EBUS practitioners, since we are going to correlate from literature the schematics with CT's

and ultrasound in every lymph node station, in order to have a detailed mental image of the mediastinum. (Figure 6).

Station 1 lymph nodes (Figure 7) are located caudal to the inferior margin of the cricoid but cranial to the incisura jugularis of the sternum and cranial to the clavicles bilaterally. Therefore, the supraclavicular nodes are also part of station 1. The latter can be felt by a clinical examination when enlarged; however, external ultrasound has shown to be useful for their localization, identification, and puncture.21–24 21 [107-110].

Although the paratracheal part of station 1 can be reached by EBUS-TBNA (1R/L; bilateral–the midline of the trachea serves as the border) or EUS-FNA (1L; left), the proposed anatomic borders cannot be recognized with endoscopic ultrasound. Because these nodes are localized extrathoracic, an endoscopic approach is very unpractical. The endoscopes are not stable for these very proximal stations making interpretation and sampling technically difficult and uncomfortable for the patient. Therefore, endoscopic ultrasound is of limited value for identification, delineation, and sampling of the paratracheally located station 1 nodes [21].



AV	Azygous vein
AO	Aorta
LN	Lymph node
PA	Pulmonary artery
SVC	Superior vena cava
RC1	Primary right carina
RIV	Right innominate vein
RUL	Right upper lobe
RLL	Right lower lobe
LCA	Left carotid artery
LC2	Secondary left carina
LUL	Left upper lobe

Figure 6. General view: CT-WLB-EBUS correlations for regional lymph nodes by IASLC system [106]

Station 2. The inferior border of station 2L is the transverse plane through the superior border of the aortic arch. For 2R, the inferior border is then the intersection of the caudal margin of the brachiocephalic vein with the right-sided border of the trachea. The sagittal plane tangent to the left tracheal wall now makes the difference between right and left. For endoscop-

http://dx.doi.org/10.5772/52748

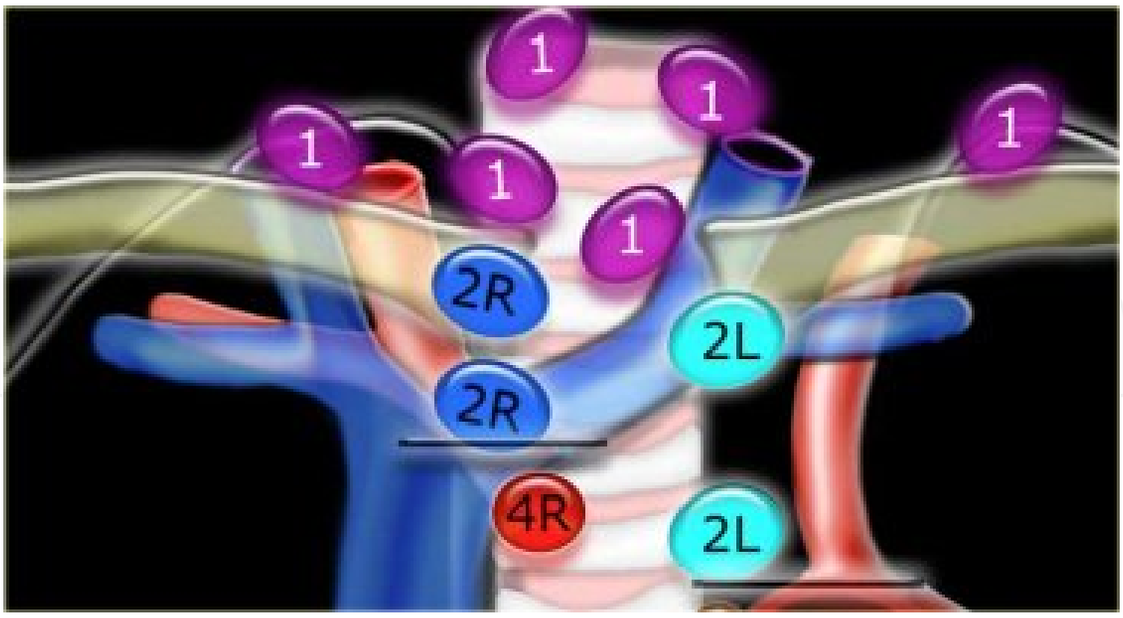


Figure 7. Supraclavicular nodes. These include low cervical, supraclavicular and sternal notch nodes. Upper border: lower margin of cricoid. Lower border: clavicles and upper border of manubrium. The midline of the trachea serves as border between 1R and 1L. 2R. Right Upper Paratracheal. 2R nodes extend to the left lateral border of the trachea. Upper border: upper border of manubrium. Lower border: intersection of caudal margin of innominate (left brachiocephalic) vein with the trachea. 2L. Left Upper Paratracheal. Upper border: upper border of manubrium. Lower border: superior border of aortic arch. [111] Courtesy of Septimiu Murgu, MD and Henri Colt,MD; Bronchoscopy International www.bronchoscopy.org

ic ultrasound node identification and delineation, these revised definitions are important. Ultrasonographic discrimination between stations 2 and 4 is evident, especially on the left side because the apex of the aortic arch can readily be visualized by either EUS-FNA or EBUS-TBNA. For the right-sided nodes, the margin simply follows this transverse plane, which can serve as a surrogate for the intersection of the trachea and brachiocephalic vein (Figure 8).

Discriminating left and right-sided nodes has clinical implications (N2 versus N3). In most of the cases, there is no discussion about the position because the presence and the size of the nodes as seen and measured on the CT scan also help the endoscopist in the identification (Figure 9). However, it can be that similarly enlarged nodes are found in this region and that attention is needed for making the difference between N2 and N3. As a general rule, it can be said that EUS-FNA can only reach the left paratracheal lymph node stations. With EBUS-TBNA, both stations can be approached while no clear endoscopic or ultrasonographic landmarks are available to discriminate left and right. Although the bronchoscopic image helps during EBUS-TBNA, the left side of the trachea never identifies as a straight plane. The large arteries (subclavian artery or the aortic arch) cannot help much because their position relative to that sagittal plane is variable. In addition, the smaller ultrasonography window of EBUS-TBNA also makes the visualization of the anatomic ultrasound landmarks is more limited [21].

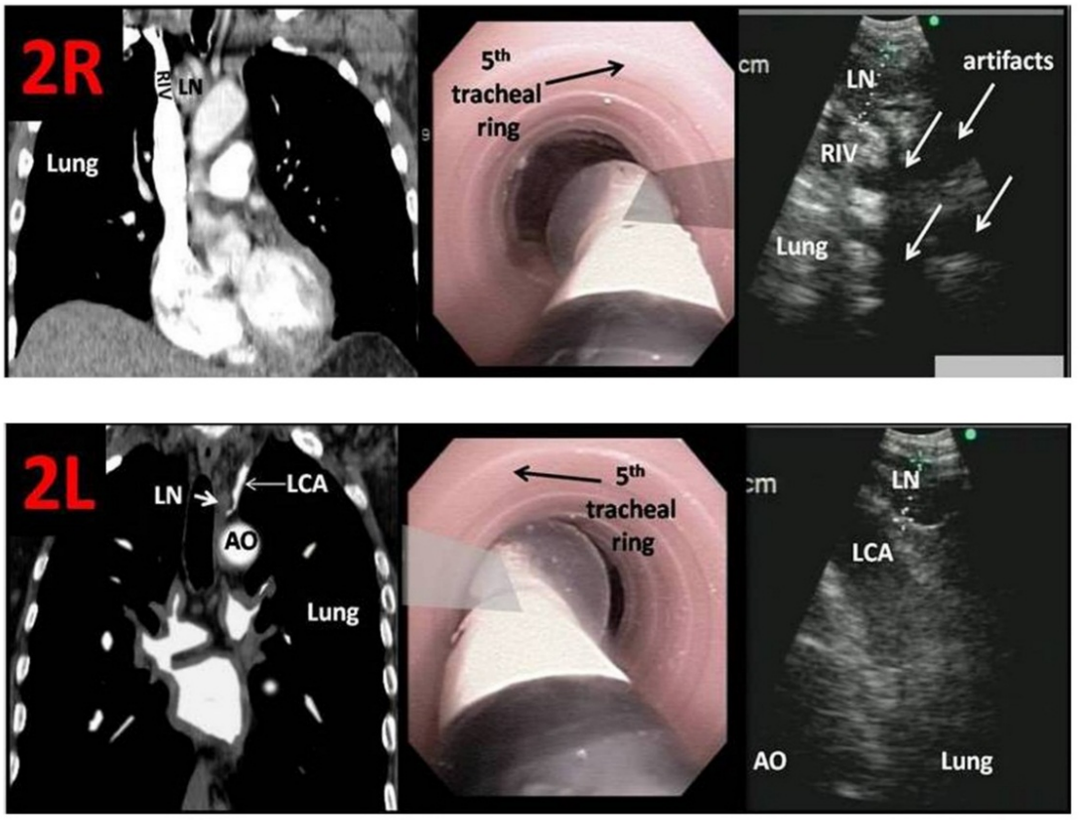


Figure 8. Station 2 visualized by EBUS at the 5th tracheal ring [106]. Courtesy of Septimiu Murgu, MD and Henri Colt,MD; Bronchoscopy International www.bronchoscopy.org

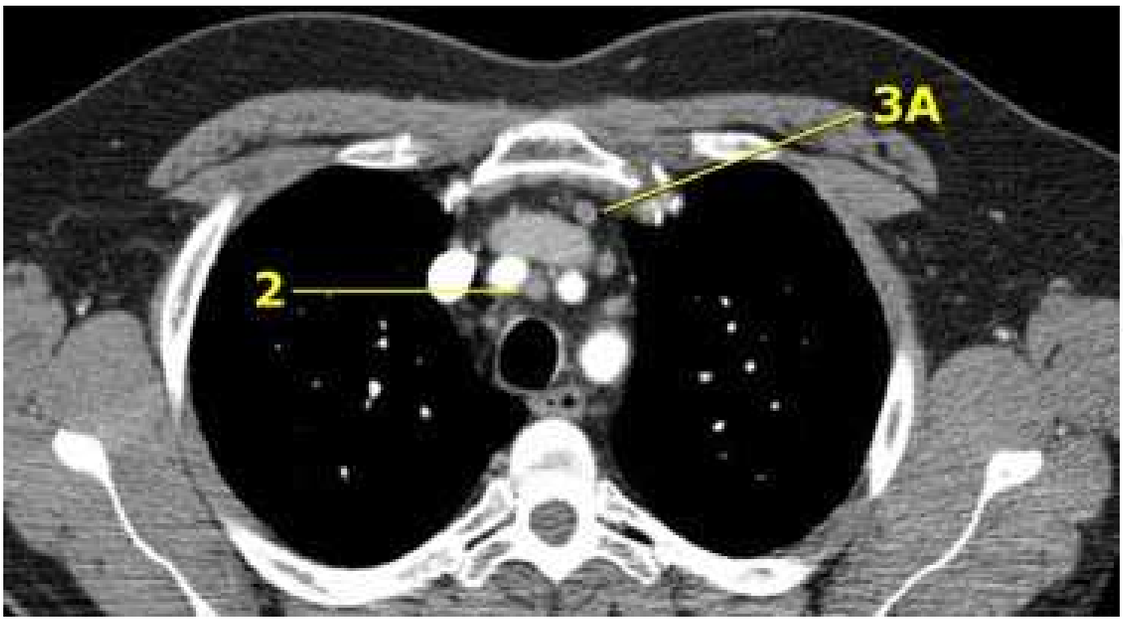


Figure 9. Station 2 node in front of the trachea, i.e. a 2R-node. There is also a small prevascular node, i.e. a station 3A node.

http://dx.doi.org/10.5772/52748

Station 3 lymph nodes are defined with an anterior part being the prevascular nodes and a posterior part being the retrotracheal nodes. The craniocaudal extent goes for both from the sternal notch down to the main carina. Although the prevascular station 3A can be visualized with EBUS as lying ventrally from the large vessels, there are no anatomic ultrasound landmarks to recognize the superior border of this lymph node station. Sampling station 3A by endoscopic ultrasound is impossible because of the interposition of the large vessels. This contrasts with station 3P, which is situated in between the pars membranacea of the trachea and the vertebrae (Figure 11). It can be seen and sampled by both EUS-FNA and EBUS-TBNA. Although there is no ultrasound landmark for the superior margin of 3P either the inferior margin being the main carina level corresponds with the level of the main stem or left pulmonary artery during EUS and can be seen as an anatomic structure during EBUS. The margin between 3P and 2/4L is the left posterior tracheal corner, which is identifiable by EUS-FNA or EBUS-TBNA. The margin between 3P and 2/4R is the right posterior tracheal corner that can be identified during EBUS-TBNA.

Station 4 lymph nodes are located paratracheally but situated caudal to the transverse aortic arch plane (Figure 12). The sagittal plane on the left side of the trachea is the margin between left and right, just like in station 2 nodes. By consequence, EUS-FNA in general cannot approach a right paratracheal node. The comments made to discriminate between 4R and 4L with EBUS-TBNA are identical to those for stations 2. However, what can be helpful for the endoscopist is that 4R nodes are situated posterior to the superior vena cava and/or ascending aorta, both presenting as large vessels with a vertical course, which can be readily visualized by EBUS-TBNA. The inferior margins of station 4 nodes have been redefined with important clinical implications, also for endoscopic ultrasound. The pleural reflection no longer serves as the border between stations 4 and 10. Station 4L has now an inferior border defined by the superior rim of the left main pulmonary artery and a lateral margin defined by the aortopulmonary ligament (Figures 12 – 14). With both EUS-FNA and EBUS-TBNA, the cranial rim of the left main pulmonary artery can be visualized. The aortopulmonary ligament is invisible for ultrasound. Station 4R's inferior border has now been redefined as the inferior border of the azygos vein. This new definition is better because the anatomic margin being the pleural fold is invisible for conventional or endoscopic imaging, whereas the azygos vein is always visible. During EBUS-TBNA, it typically presents in the right tracheobronchial corner as a kidney-shaped vessel (Figures 12, 13). By consequence, EBUS-TBNA now can be used more confidently to discriminate between mediastinal 4R and hilar 10R nodes. The 4R nodes are by consequence characterized by their position just dorsally from the superior caval vein and/or aorta and medially but not distally to the azygos vein.

4R. Right Lower Paratracheal

- Upper border: intersection of caudal margin of innominate (left brachiocephalic) vein with the trachea.
- Lower border:lower border of azygos vein.

4R nodes extend to the left lateral border of the trachea.

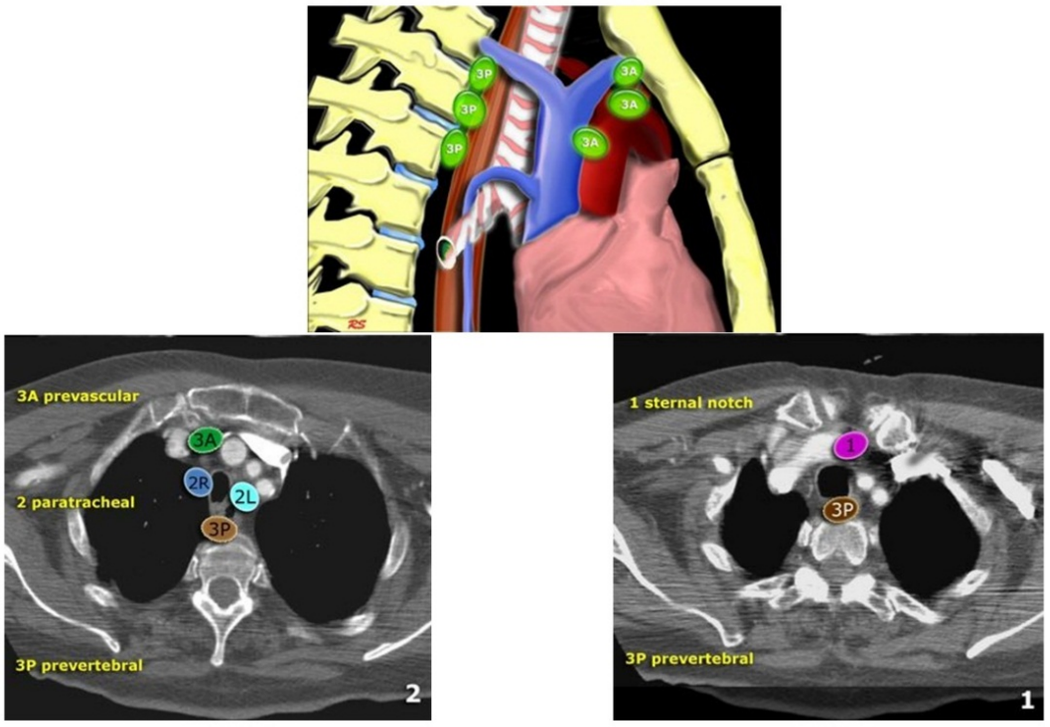


Figure 10. Prevascular and Prevertabral nodes. Station 3 nodes are not adjacent to the trachea like station 2 nodes. They are either: 3A anterior to the vessels or 3P behind the esophagus, which lies prevertebrally. Station 3 nodes are not accessible with mediastinoscopy. 3P nodes can be accessible with endoscopic ultrasound (EUS) [111].

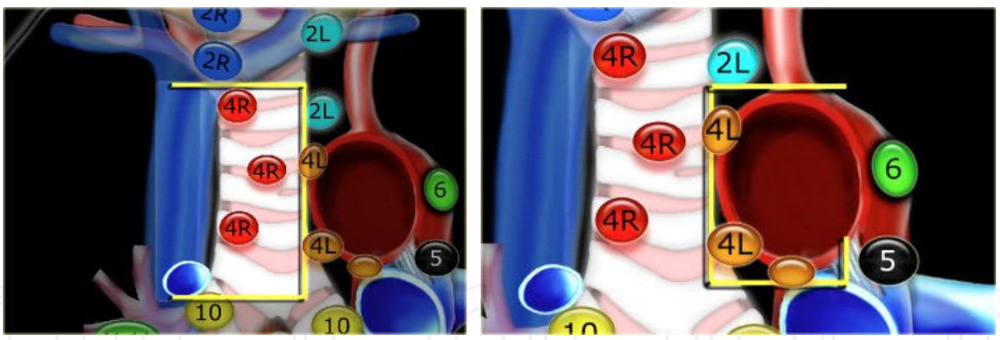


Figure 11. Lymph nodes station 4 and their borders

4L. Left Lower Paratracheal

4L nodes are lower paratracheal nodes that are located to the left of the left tracheal border, between a horizontal line drawn tangentially to the upper margin of the aortic arch and a line extending across the left main bronchus at the level of the upper margin of the left upper lobe bronchus. These include paratracheal nodes that are located medially to the ligamentum arteriosum.

Station 5 (AP-window) nodes are located laterally to the ligamentum arteriosum [111].

http://dx.doi.org/10.5772/52748

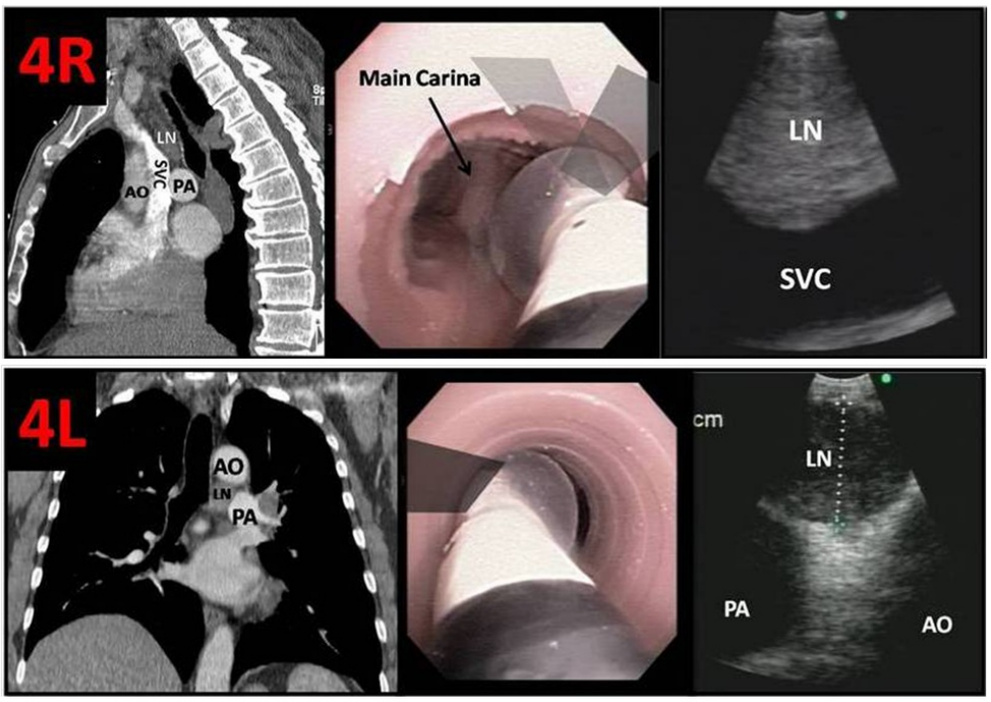


Figure 12. Sagital CT, bronchoscopic image and EBUS image of station 4R and 4L lymph node stations [106]. Courtesy of Septimiu Murgu, MD and Henri Colt,MD; Bronchoscopy International www.bronchoscopy.org

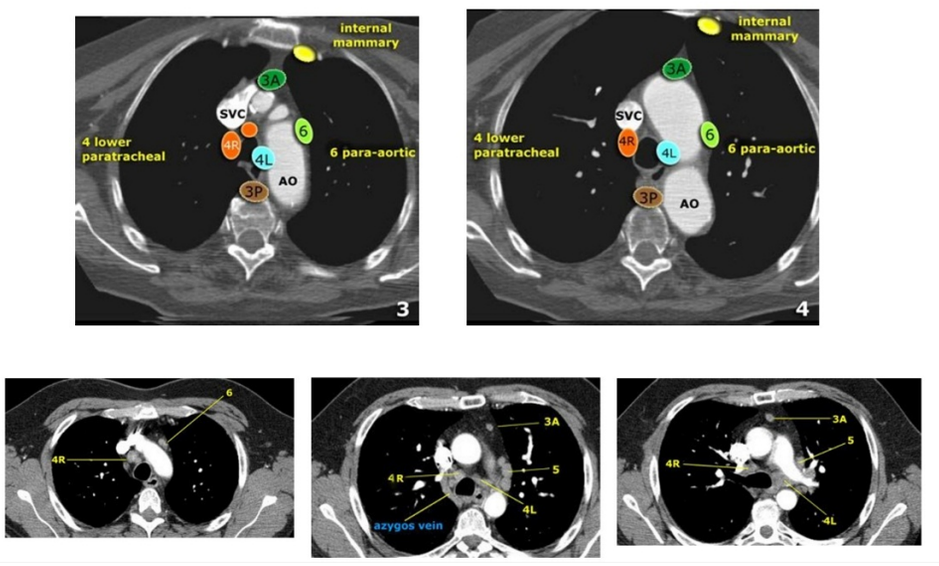


Figure 13. Examples of mediastinal lymph nodes and their anatomic relations with described borders [111].

Station 5 lymph nodes are situated laterally to station 4L nodes with the ligamentum arteriosum as anatomic border (Figures 11, 13). The inferior edge is similar for both, whereas the cranial edge is not. Although 4L nodes are situated caudal to the superior border of the aortic arch, station 5 nodes are located caudal to the inferior border of the aortic arch (Figure 19).

Because the ligamentum arteriosum cannot be discerned by means of ultrasound, the differentiation between 4L and 5 can be difficult, especially when both stations contain suspect lymph nodes. Station 5 nodes can be identified by EUS-FNA and EBUS-TBNA although the latter is often more demanding. Because of the interposition of aortic arch or pulmonary artery, station 5 can only be punctured in selected patients with enlarged nodes.

Station 6 mediastinal lymph nodes are located lateral to the ascending aorta and aortic arch, in between the transverse planes at the superior and inferior border of the aortic arch. (Figures 13, 14) These nodes can most often be identified by means of EUS-FNA, whereas this is not always possible with EBUS-TBNA. The nodes in station 6 can only be punctured by a transaortal approach, but extended mediastinoscopy is advised instead [21, 112].

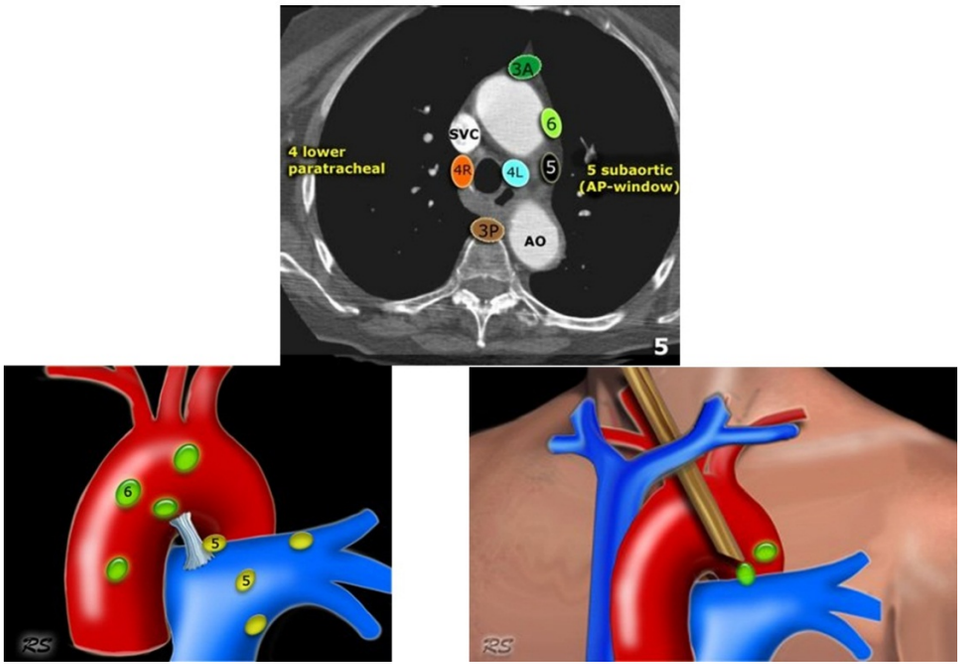


Figure 14. Lymph nodes stations 5 and 6 and their relation with the great vessels [111].

Station 5. Subaortic nodes: Subaortic or aorto-pulmonary window nodes are lateral to the ligamentum arteriosum or the aorta or left pulmonary artery and proximal to the first branch of the left pulmonary artery and lie within the mediastinal pleural envelope.

Station 6. Para-aortic nodes: Para-aortic (ascending aorta or phrenic) nodes are located anteriorly and laterally to the ascending aorta and the aortic arch from the upper margin to the lower margin of the aortic arch [111].

Station 7 lymph nodes have an inferior border that is redefined. (Figure 15).On the left side, this is the superior border of the lower lobe bronchus, and on the right side, this is the inferior border of the intermediate bronchus. (Figure 16) The lymph nodes in this station can be seen and biopsied by both EUS-FNA and EBUS-TBNA. Formerly, an anterior and posterior part of this node was recognized. This was meaningful because a cervical mediastinoscopy

http://dx.doi.org/10.5772/52748

cannot reach the posterior part of this station. With EUS-FNA and EBUS-TBNA, the entire subcarinal area can be approached. Although identification of the nodes in this station is easy for both EUS-FNA (the nodes lay just dorsally to the origin of the left pulmonary artery and cranial to the left atrium) and EBUS-TBNA (by means of the endoscopic view), the delineation of the inferior border by means of endoscopic ultrasound is, however, not easy. With EUS-FNA, the left atrium is generally seen as the anatomic border above which the subcarinal nodes are situated, although this is with the new definition probably too restrictive. The relation of the left atrium or pulmonary artery to the bronchus intermedius and the left lower lobe bronchus, the latter being the newly defined inferior borders of station 7, can be variable. With EBUS-TBNA, the delineation of the inferior border is possible because this investigation allows a simultaneous bronchoscopic view of the bronchial tree although there are no distinct corresponding ultrasound landmarks.

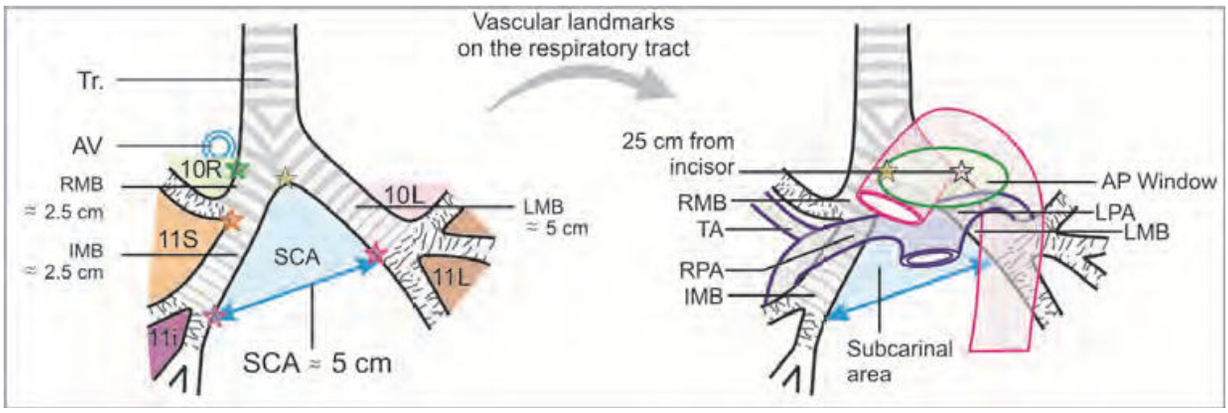


Figure 15. Virtual borders between lymph node stations and their relation with the great vessels of mediastinum [113].

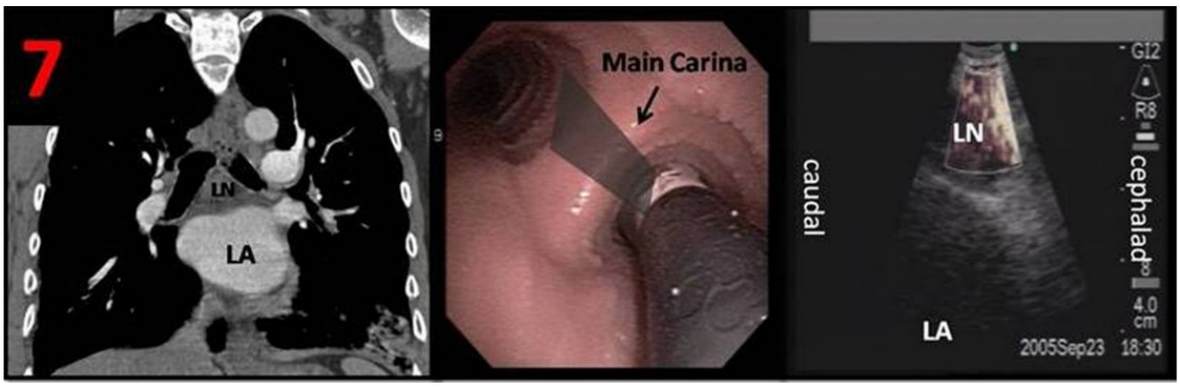


Figure 16. The subcarinal station shown on CT scan (left panel) can easily be visualized with both EUS (right panel) but of course also with EBUS. During EUS, the subcarinal station identifies as a round, hypoechogenic sharply edged structure located in between the esophagus and the pulmonary artery. The upper rim of this artery corresponds in general with the main carina and is helpful during EUS. The main carina is visualized by means of endoscopy during EBUS. The inferior border is the roof of the lower lobe bronchus on the left and the bottom of the bronchus intermedius on the right. There are no unique ultrasound features that correspond to this definition although endoscopy during EBUS is helpful [21]. Courtesy of Septimiu Murgu, MD and Henri Colt,MD; Bronchoscopy International www.bronchoscopy.org

Stations 8 and 9 are the paraoesophageal and pulmonary ligament nodes, respectively, and are situated inferior to the inferior margins of station 7 lymph nodes. The superior border of these lymph nodes is as such defined by the inferior margin of the subcarinal area. Station 8 nodes are located along the left atrium (Figures 17, 18), whereas station 9 nodes are lying within the pulmonary ligament (Figure 19). Although the latter is a structure that cannot be seen with endoscopic ultrasound, station 9 nodes are located just cranial to the diaphragm, which is readily identifiable with EUS-FNA. Stations 8 and 9 lymph nodes can be thus approached by means of EUS-FNA. Occasionally, station 8 nodes can be found by EBUS-TBNA. However, and as suggested above, one has to take into account the inferior stretch of the subcarinal nodes making this station in addition to station 9 becomes invisible for EBUS-TBNA. When performing EUS-FNA, one cannot confuse a lesion or lymph node with the esophagus. When performing EBUSTBNA, the esophagus can be seen as a multilayered structure with a hyperechogenic line in the middle corresponding with air not to be misinterpreted as a lymph node. The discrimination between the left- and right-sided nodes is the midline. Although no formal ultrasound characteristics for the midline are available, the relative position of the endoscope to the descending aorta can help.

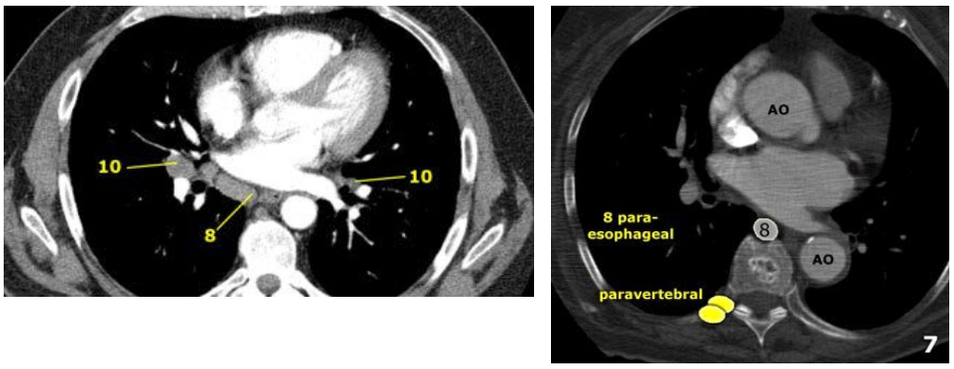


Figure 17. Station 8 Paraesophageal nodes: these nodes are below the carinal nodes and extend caudally to the diafragm. On the left an image below the carina. To the right of the esophagus a station 8 node [111].



Figure 18. Station 9. Pulmonary ligament nodes: pulmonary ligament nodes are lying within the pulmonary ligament, including those in the posterior wall and lower part of the inferior pulmonary vein. The pulmonary ligament is the inferior extension of the mediastinal pleural reflections that surround the hila [111].

http://dx.doi.org/10.5772/52748

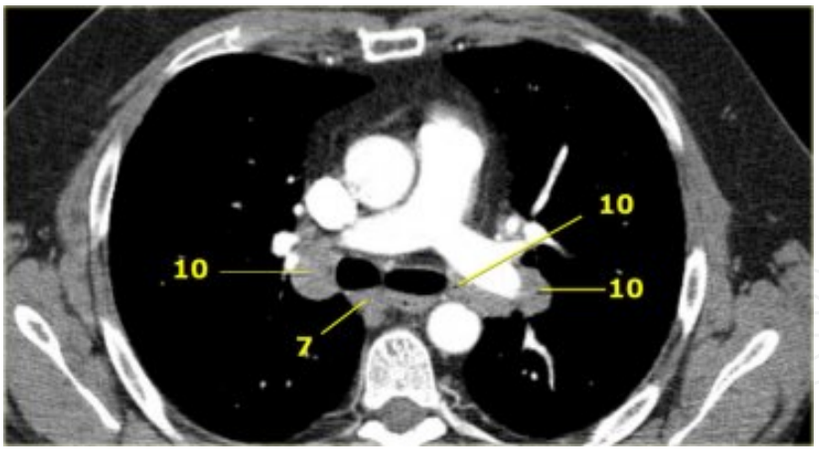


Figure 19. Hilar nodes Hilar nodes are proximal lobar nodes, distal to the mediastinal pleural reflection and nodes adjacent to the intermediate bronchus on the right. Nodes in station 10 - 14 are all N1-nodes, since they are not located in the mediastinum [111].

Station 10 or hilar lymph nodes are situated immediately adjacent to the main stem bronchus but caudal to the inferior border of azygos vein on the right and superior rim pulmonary veins and artery on the left. These nodes can be seen and sampled by EBUS-TBNA (Figures 20, 21). The inferior margin of station 10R is the interlobar region. There is no unique ultrasound feature that defines that border, but because a bronchoscopic view is available during EBUS-TBNA, the secondary carina or the upper lobe split off can serve as surrogate here. EUS-FNA has been thought to be unable to see and sample hilar stations. However, there is no doubt that in certain cases, station 10 nodes located medially from the main stem bronchi can be assessed. Endoscopists should be aware of this because misinterpretation could lead to overstaging [114].

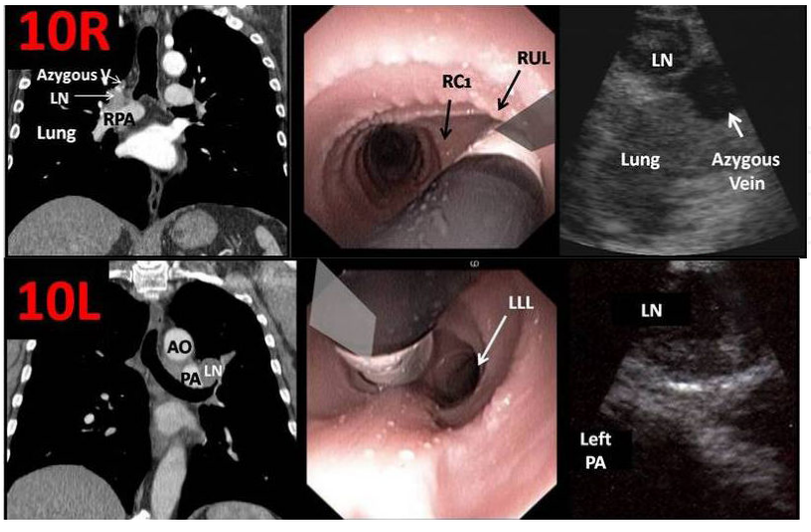


Figure 20. Station 10 lymph nodes: sagittal CT, endobronchial view and corresponding EBUS [106]. Courtesy of Septimiu Murgu, MD and Henri Colt,MD; Bronchoscopy International www.bronchoscopy.org

Once the secondary carina is reached, station 11 lymph nodes (or interlobar nodes) are encountered. From this station on, the nodes can only be approached by EBUS-TBNA and not by EUS-FNA. These nodes are located just underneath the mucosa of the secondary carina on the left. There is a division between 11s and 11i on the right side. The former indicate the nodes between upper lobe and intermediate bronchus, the latter are situated in between middle and lower lobe ultrasound landmarks are not available; however, the synchronous endoscopic view enables the identification of the relevant lobe split offs.

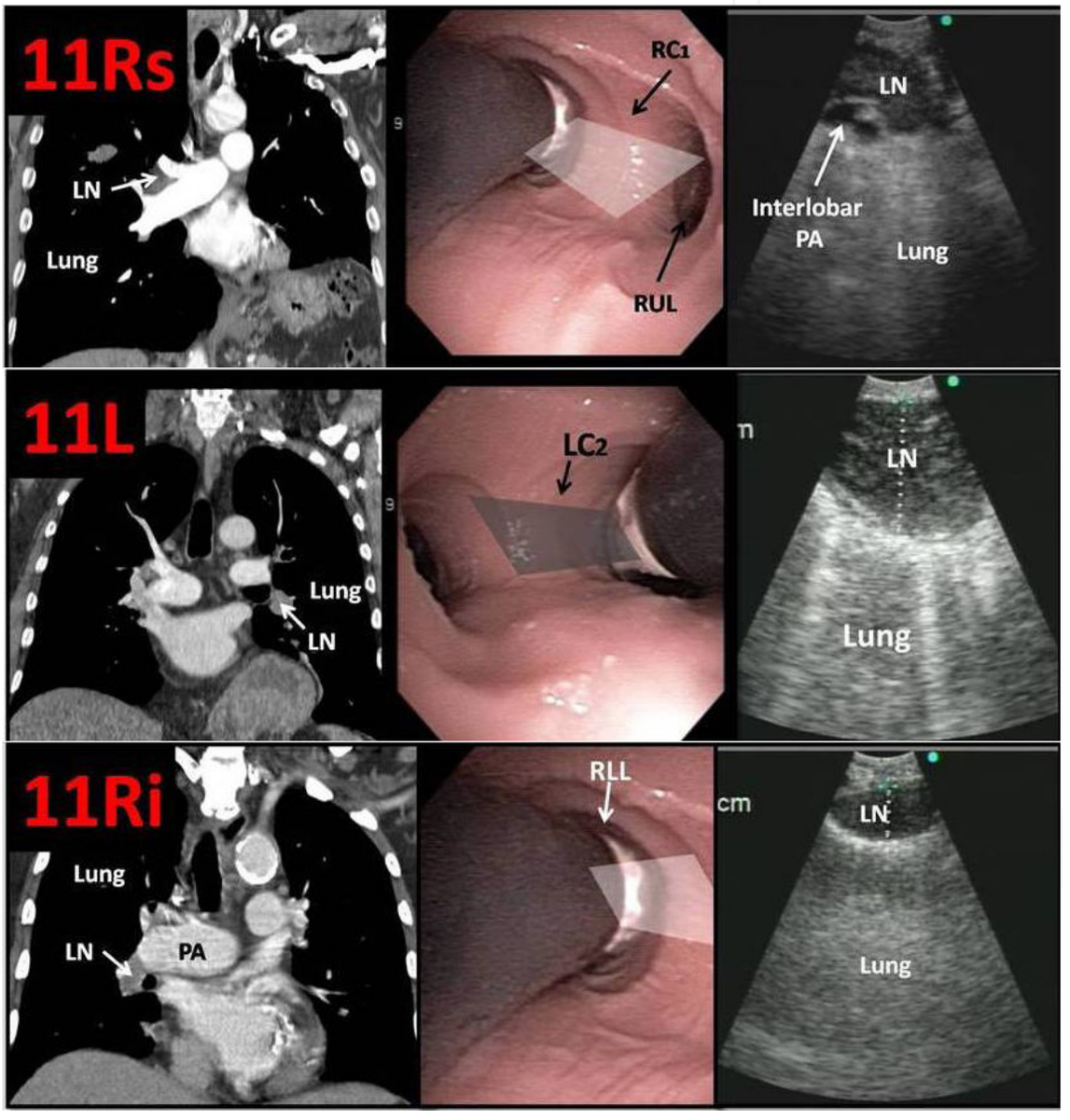


Figure 21. Station 11 lymph nodes (hilar nodes): Sagittal CT, endoscopic view and corresponding EBUS [106]. Courtesy of Septimiu Murgu, MD and Henri Colt,MD; Bronchoscopy International www.bronchoscopy.org

Once the lobar bronchi originate, then **station 12** is reached. Again, there are no unique ultrasound borders, only the endoscopic view can help for guidance. **Stations 13 and 14** are segmental and subsegmental nodes. Frequently, the EBUS-TBNA endoscope is too large to approach the segments and subsegments and their lymph nodes.

In closing, the new IASLC map maintains the lymph node stations of the other maps, but it also groups those that are anatomically proximal in lymph node areas in order to make the lymph node classification easier, especially in patients who will not undergo surgery. In this map, all the lymph node stations are defined by anatomically precise limits that are easy to recognize with imaging techniques and inspection during invasive explorations or thoracotomy. The innovations of this lymph node map are:

- The creation of a supraclavicular lymph node area that includes the supraclavicular, lower cervical (caudal on the lower edge of the cricoid cartilage) and the suprasternal fossa lymph nodes. If these lymph nodes are invaded by a tumor, they are classified as N3, regardless of the side of the tumor.
- The widening of the subcarinal lymph node station. It now includes all the lymph nodes from the tracheal bifurcation until the upper edge of the lower left lobar bronchus and the lower edge of the intermediary bronchus. If they are affected by tumors, these lymph nodes are classified as N2. This new subcarinal station includes lymph nodes that before, at least according to the Japanese map, were hilar (adjacent to the lower sides of the main bronchi), that could be classified as N1 or N3, depending on the side of the tumor. The larger size of this subcarinal station will mean an increase in N2 tumors in detriment of N1 and N3 tumors.
- The incorporation of precise limits for station number 10, the hilar station, which facilitates the prospective collection of data in order to clarify the prognostic role of this station, whose placement on other maps has always been controversial.
- The shift in the midline of the upper mediastinum from the tracheal anatomical midline to the left paratracheal margin exclusively affects the upper and lower right and left paratracheal stations. This modification implies that the affected lymph nodes that are to the left of the anatomical midline, but to the right of the new left paratracheal line, will be N2 for tumors of the right lung, but N3 for those of the left lung.

1.4. Changes to M descriptors [25, 39]

The patients with lung cancer studied for the 7th edition of the TNM Classification of Malignant Tumors presented the following survival rates at 1 and 5 years: T4 any N M0, 53% and 16%; pleural dissemination, 45% and 6%; contralateral pulmonary nodule(s), 46% and 3%, and distant metastasis, 22% and 1%; in this latter case, with significantly lower survival rates than previously cited [39]. With such references, it was decided to subdivide the M component into M1a (presence of pleural dissemination or contralateral pulmonary nodule(s)) and M1b (distant metastasis).

Subclassify the M1 component in (Table 7):

- M1a: Intrathoracic metastasis.
- M1b: Extrathoracic (distant) metastasis.
- Reclassify pleural dissemination (malignant pleural effusions, pleural nodules) and malignant pericardial effusions as a metastasis descriptor: from T4 to M1a.
- Subclassify M1 by additional nodules in the contralateral lung as M1a.
- Subclassify M1 by distant metastases as M1b.
- The MX and pM0 designation has been eliminated from the AJCC/UICC TNM system.

M factor definitions	6th ed descriptor	7th ed descriptor
Metastasis cannot be assessed.	MX	M0
Malignant pericardial effusion.	T4	M1a
Pleural dissemination (malignant pleural effusions, pleural nodules).	T4	M1a
Additional nodules in the contralateral lung (same histology).	M1	M1a
Distant metastasis.	M1	M1b

Table 7. M descriptor changes: comparison between 6th and 7th edition of the TNM Classification of Malignant Tumors [39].

1.4.1. Additional changes

- Introduction of a new accurate definition of visceral pleural invasion (VPI); VPI is a pT2 descriptor (Table 8). To avoid confusion, the abbreviation PL is employed instead of P which is also used for designation of pTNM in distinction from cTNM. The IASLC also recommends the use of elastic stains to distinguish between PL0 and PL1 when hematoxylin and eosin (H&E) sections are not helpful [71].

PL category	Definition	T status	
PL0	Tumor within the subpleural parenchyma or, invading superficially into the pleural connective tissue below the elastic layer.	PL0 is not a T descriptor and the T component should be assigned on other features.	
PL1	Tumor invades beyond the elastic layer.	pT2	Indicates VPI
PL2	Tumor invades to visceral pleural surface.		
PL3	Tumor invades the parietal pleura.	pT3	

Table 8. Classification of visceral pleural invasion (VPI): Proposed modification of Hammar Classification [115]

- Clinical TNM staging now is valid for SCLC, and stratification by stage I to III should be included in clinical trials of early stage disease [116].
- Pathologic TNM staging must be used for all SCLC cases [117]..The International Staging Committee of the IASLC has confirmed that the survival of patients with SCLC worsened as the T and N categories increased [116]. It was also observed that, except in stage IIA, which had only 55 patients for analysis, the 5-year survival worsened as the stage progressed: IA, 38%; IB, 21%; IIA, 38%; IIB, 18%; IIIA, 13%; IIIB, 9%, and IV, 1%. Based on this, the proposal to use the TNM system for staging SCLC was confirmed.
- Carcinoid tumors are now included within the TNM classification [118], a new staging system for neuroendocrine tumors. Lung carcinoids are staged in the same way as carcinomas.

Even though the 6th TNM classification specified that it was not applicable to carcinoid tumors, several studies have used it, finding prognostic differences among the stages. The IASLC has also confirmed that those classified as stage I lived significantly more than those in stage II, and these significantly more than those in stages III–IV; therefore, the new TNM classification of 2009 is recommended to describe the extension of these tumors [118].

Knowing the previous arguments for reorganizing some sections of the T and M components, a sophisticated statistical study was carried out with 17,726 patients whose tumors were better staged [119]. The different survival curves for each stage were obtained, which, without overlapping among them, presented worse levels as the tumor extension increased. This confirms the new stage grouping (Table 9), whose 5-year survivals for each stage were, according to clinical and pathological staging, respectively, the following: IA, 50% and 73%; IB, 43% and 58%; IIA, 36% and 46%; IIB, 25% and 36%; IIIA, 19% and 24%; IIIB, 7% and 9%, and IV, 2% and 13%.

6th ed	7th ed	N0	N1	N2	N3
T/M descriptors					
T1 (=2cm)	T1a	IA	IIA	IIIA	IIIB
T1 (>2 cm =3 cm)	T1b	IA	IIA	IIIA	IIIB
T2 (>3 cm =5 cm)	T2a	IB	IIA(IIB)	IIIA	IIIB
T2 (>5 cm = 7 cm)	T2b	IIA	IIB	IIIA	IIIB
T2 (>7 cm)	T3	IIB(IB)	IIIA(IIB)	IIIA	IIIB
T3 (direct invasion)		IIB	IIIA	IIIA	IIIB
T4 (same lobe nodules)		IIIB(IIIA)	IIIA(IIIB)	IIIA(IIIB)	IIIB
T4 (extension)	T4	IIIA(IIIB)	IIIA(IIIB)	IIIB	IIIB
M1 (ipsilateral nodules)		IIIA(IV)	IIIA(IV)	IIIB(IV)	IIIB(IV)
T4 (pleural or pericardial effusion)	M1a	IV(IIIB)	IV(IIIB)	IV(IIIB)	IV(IIIB)
M1 (contralateral nodules)		IV	IV	IV	IV
M1 (distant)	M1b	IV	IV	IV	IV

Table 9. Stage Grouping Comparisons: Sixth Edition Versus Seventh Edition Descriptors, T and M Categories, and Stage Groupings.

Cells in bold indicate a change in the stage from the sixth edition. Adjacent stage in parentheses represents staging from the sixth edition. T = primary tumor; N0 = no regional lymph node metastasis; N1 = metastasis in ipsilateral peribronchial and/or ipsilateral hilar lymph nodes and intrapulmonary nodes, including involvement by direct extension; N2 = metastasis in ipsilateral mediastinal and/or subcarinal lymph node(s); N3 = metastasis in contralateral mediastinal, contralateral hilar, ipsilateral or contralateral scalene, or supraclavicular lymph node(s); M = distant metastasis [65].

Stage groupings were modified due to changes to the TNM descriptors (Table 5).

1. TNM grouping categories that were down-staged:
   - **a.** T2 smaller tumors, now T2a (>3 cm =5 cm), N1M0 are down-staged from IIB to IIA.
   - **b.** T4 tumors due to additional nodules in primary lobe, now T3, are down-staged from IIIB to IIB (N0) or to IIIA (N1-2).
   - **c.** M1 cases due to additional nodules in other ipsilateral lobe(s), now T4, are down-staged from IV to IIIB (N2-3) or to IIIA (N0-1).
   - **d.** T4 tumors due to other factors, N0-1 are down-staged from IIIB to IIIA.
2. TNM grouping categories that were up-staged:
   - **a.** T2 larger tumors, now T2b (>5 cm =7 cm), N0M0 are up-staged from IB to IIA.
   - **b.** T2 tumors >7 cm, now T3, are up-staged: T3N0M0 from IB to IIB and T3N1M0 from IIB to IIIA.
   - **c.** Tumors with pleural nodules or malignant pleural (or pericardial) effusion were reclassified from T4 to M1a, therefore are up-staged from stage IIIB to IV [120].

The main limitations are derived from the retrospective character of some databases that were not designed to study the TNM classification and lack precise anatomical details about the tumor extension, the number and lymph node stations affected or the differences between the different forms of M1 disease. For this reason, the IASLC itself has initiated a prospective project aimed at once again updating the TNM classification in 2016, validating all the T, N and M descriptors, especially those who have not been until now. Thus, a large international database is being constituted that, correcting the geographical omissions and disproportions in the therapeutic modalities, includes patients with non-small-cell tumors, small-cell tumors and their neuroendocrine subtypes.

In conclusion, the IASLC staging classification is unquestionably a major advance. The size of the database, the broad international spectrum, the careful and detailed analysis, as well as the internal and external validation, are tremendous achievements and relatively unique among types of cancer [121].

So, the main advantages of the new classification would be:

- The size of the database, the largest ever collected for any cancer type.
- For the first time, data was collected from different countries.

- The timeframe of 10 years allowed for 5 years follow-up.
- Cases included all treatment modalities.
- Pathologic and clinical staging where considered in survival analysis.
- The statistical analysis included meticulous internal and external validation.
- Changes to the TNM descriptors and stage groups were derived strictly from the outcome measure of overall survival.

The new TNM system is less intuitive and more complex than the 6th edition, and will be more difficult to learn. The oncology community needs to overcome the higher learning curve in order to offer patients the most appropriate treatment choices based on more accurate prognostic information [120].

2. Electromagnetic navigation bronchoscopy

It is known that diagnostic yield of flexible bronchoscopy is limited by its inability to guide biopsy instruments directly to the lesion. As it was expected, diagnosis success rate is dependent on the size and location of the lesion. The diagnostic yield of flexible bronchoscopy is expected to be between 20 and 84%. However, current nonsurgical techniques available to diagnose small peripheral lung lesions (SPLL) are limited either by low accuracy [122–125] or by potential complications [126–129].

For lesions less than 2 cm in diameter, the diagnostic yield of flexible bronchoscopy is 14% for peripheral lesions in the outer third of the chest and as high as 31% if in the proximal two-thirds [130]. The diagnostic yield of flexible bronchoscopy for mediastinal lymph nodes using transbronchial needle aspiration (TBNA) is reported to be between 15 and 83% [131]. Also, diagnostic yield of TBNA in staging of bronchogenic carcinoma is reported to be between 50 and 60% [132].

Within the past several years, electromagnetic navigation guided bronchoscopy (EGB) has proven very effective at assessing pulmonary nodules accurately with very low complication rates. EGB consists of four elements:

1. Computer software that utilizes thin-slice CT to create a three-dimensional rendering of the lung and tracheobronchial tree, which can then be used for virtual bronchoscopy.
2. A sensor probe that fits through the small working/suction channel of a bronchoscope with a steering mechanism. Because the sensor probe is recognizable within the electromagnetic field, it can be navigated through the small airways of the lung toward peripheral lesions not reachable by conventional bronchoscopy (Figure 22).
3. An electromagnetic field encompassing the patient's thorax, so that the real anatomy can be merged with the computer generated (virtual) anatomy by use of standard "registration points" (e.g., carina, takeoff of the right upper lobe bronchus, bifurcation between the left upper and lower lobes).

4. A hollow, extended working channel (EWC) that can be secured in a small peripheral airway and used to pass diagnostic instruments such as brushes, aspirating needles and biopsy forceps [133].

The ideal patient for EGB should be one with peripheral pulmonary lesion (solid or fatty solid nodule located beyond the visible range of flexible bronchoscopy) detected by chest radiography and CT or presenting with suspicion of cancer by CT morphology or positive positron emission tomography (PET) scan, as well as with a nondiagnostic conventional bronchoscopy in most of these cases; he should have absence of other metastatic lesions accessible for biopsy, a negative TTNA or contraindication for TTNA (severe pulmonary impairment, bleeding diathesis, lesions not accessible by TTNA as judged by a radiologist panel) and contraindication for straightforward curative surgery; in case of associated mediastinal lymph nodes should have a negative transbronchial needle aspiration (TBNA) or difficult to reach with TBNA lymph nodes.

Those patients who should not undergo EGB are those with contraindication to short-acting anesthetic agents, bleeding diathesis, presence of concomitant endobronchial lesion, presence of a pacemaker/defibrillator or a diagnosis by other means (sputum cytology, microbiology) that offers a reliable and easy to control course of treatment.

Navigation aim is to closely approach the target lesion (distance between sensor tip and lesion centre ≤15 mm) and take as many biopsies as possible for each lesion. At every three attempts is advised that the forceps should be withdrawn and the position of the sensor probe in relation to the target lesion checked.

Makris D et al. also recommends that all patients should undertake a CT scan prior to EGB with the following technical criteria: slice thickness 2–3.5 mm, interval between slices (with overlap of 1 mm) 1-2.5 mm, image size 512x512 pixels and dicom format [134].

As for anesthesia, Gildea TR et al. considers that all procedures (flexible bronchoscopy, bronchial washings, bronchoalveolar lavage and the actual EGB) can be safely performed using conscious sedation with intravenous 2 mg boluses of both midazolam and morphine with topical lidocaine [135].

In an emblematic study from Gildea TR et al. in 2006, the role of electromagnetic navigation bronchoscopy using super-Dimension/Bronchus System as a novel method to increase diagnostic yield of peripheral and mediastinal lung lesions was investigated. The superDimension/bronchus system is an image-guided localization system, which is designed to guide bronchoscopic tools to predetermined points within the bronchial tree. The device uses three separate technologies that are combined to enable navigation of dedicated tools within the lung in real time.

The first component is the planning software, which converts digital imaging and communications in medicine standards (DICOM) images from a computed tomography (CT) scan into multiplanar images with three-dimensional reconstruction and virtual bronchoscopy of the airways.

http://dx.doi.org/10.5772/52748

The second component is a steerable probe that contains a position sensor attached to an eight-way steerable instrument that has the ability to navigate turns in the endobronchial tree [135].



Figure 22. The steerable probe (SP) with bronchoscope [18].

The third component is an electromagnetic (EM) board, which is a field generator connected to a computer containing the planning data. The exact position of the steerable probe when placed within the EM field is depicted on the system monitor.

Registration is the process by which the computer links the five to six virtual fiducial markers to the actual position in the patient. Upon registration completion, the average fiducial target registration error (AFTRE) score was given in millimetres (mm). The AFTRE is the radius of expected difference of the location of the tip of the steerable probe in the actual patient compared with where it is expected to be in the virtual patient [135].

After registration, navigation is performed with simultaneous advancement of the steerable probe toward the target and directing steerable probe to the lesion. The closest distance between the steerable probe tip and the lesion centre is recorded. When navigation is completed, the steerable probe is removed, leaving the extendable working channel through which brushings and TBBXs or TBNA were performed [135].

In this study, biopsies were performed using a C-arm fluoroscopy unit. All instruments were visualized under fluoroscopy only after navigation was completed to confirm proper function and position of the bronchoscopic tools relative to the lesion and the pleura. Brush biopsies involved two to three passes, and four pieces of tissue were obtained by TBBX. TBNA usually was done with 2 to 4 passes of a combination of 19-G and 22-G needles depending on physician choice [130, 135-139].

Eberhardt et al. [18] reported in 2007 92 peripheral lung lesions biopsies from 89 consecutive subjects. The diagnostic yield of EGB was 67%, which was independent of lesion size. Total procedure time ranged from 16.3 to 45.0 min (mean [± SD] procedure time, 26.9 ± 6.5 min). The mean navigation error was 9 ± 6 mm(range, 1 to 31 mm). They reported two incidences of pneumothorax for which no intervention was required. When analyzed by lobar distribution, there was a trend toward a higher ENB yield in diagnosing lesions in the right middle lobe (88%). They concluded that EGB can be used as an independent bronchoscopic technique without the need for fluoroscopy when compared with other available studies. There was no increased risk of pneumothorax (2 of 89 patients; 2%). The upper lobes tend to have sharper angles in the bronchial tree that may be challenging to navigate even with a steerable sensor probe. The EWC ends close to the tip of the sensor probe and makes it less flexible. This reduces the range of deflection and, consequently, the ability to navigate. It can also make the probe flip into a different position when negotiating some tight angles in the bronchi. Navigation in the lower lobes is more affected by diaphragmatic movement during breathing and could result in larger errors than recorded. This is because the planning data are based on CT scan images acquired in a single breathhold [140, 141].

Eberhardt et al. also showed that the improved yield of EGB compared to conventional transbronchial lung biopsy in small lesions (diameter ≤ 2 cm) can be attributed to the improved precision in navigation. This study has shown the yield, safety, and timesaving with use of the EGB system without the need for fluoroscopy. This system eliminates radiation exposure and could reduce procedure costs. The diagnostic utility of the use of EGB in the biopsy of peripheral lung lesions appears to be equivalent to other advanced techniques like endobronchial ultrasound [142-144].

Apparently, these techniques have pushed bronchoscopic biopsy yields closer to those achieved by CT scan-guided transthoracic needle biopsy and surgery. Given the relative comfort [145] and safety [146] of flexible bronchoscopy, and the recognized risks of both CT scan-guided [147-149] and surgical biopsies [150], there is growing need to develop and refine these techniques. The expanded role of lung cancer screening, in which the vast majority of lesions is benign, makes this all the more important [151]. Multimodality diagnosis by combining ENB with other bronchoscopic and imaging techniques may further enhance the diagnostic yield [140].

3. Autoflorescence Bronchoscopy (AFB)

Visible light perceived by the human eye comprises the whole wavelength range, between 400–700 nm. Conventional bronchoscopy illuminates mucosal structures of the airwaves with the full wave spectrum; therefore, light gets reflected, backscattered or absorbed by the structures it encounters, thus providing the human eye with an image [152]. Tissues show a natural autoflorescence when excited in the 200-460 nm range; however, only the visible part of this range is used in medical applications [153].

However, the light source attached to the bronchoscope can emit only blue light, as a proportion of the blue spectrum excites the cellular chromophores, such as collagen, elastin or keratin, contained in the layers of the submucosa, especially within the connective tissue comprised in the elastic fiber bundles, or on the exterior surface of the cartilages (perichondrium). When excited by blue-violet light in the 400-450 nm spectrum, the excited chromophores of normal cellular lines found in the mucosa display a green tint. Another aspect of the autoflorescence theory refers to the thickness and cellular morphology of the examined tissue. Tumors and premalignant lesions have an increased mucosal thickness and therefore absorb more of the excitation occurring from fluorescence light, in what is called "the architectural effect" [153, 154]. Tissues that underwent a morphological change due to various pathological conditions, predominantly premalignant dysplasia or metaplasia-like phenomenon, are colored differently as the green fluorescence is affected by either alterations of cellular chemistry, morphology or epithelial thickness [155–157]. A wide range of AFB devices are currently available on the market: the Storz D-light system [158], Pentax SAFE-1000 [159], the Xilix LIFE system [158] or the DAFE system by Richard Wolf [160].

The main advantage of AFB is that progressive dysplasia of the mucosal layers also results in a progressive transition from normal green autoflorescence to a red-brown color, specific to precancerous or malignant lesions. This makes early premalignant lesions far easier to spot during bronchoscopy as compared to regular white-light based techniques. Inflammatory reactions, granulomas, scars, dysplasia/metaplasia and early malignant lesions which are hard to spot due to their submucosal confinement are therefore easily spotted due to their dark red-brown appearance, surrounded by normal green tissue [155–157].

The addition of AFB to conventional endoscopy can significantly increase diagnostic rate of early malignant or premalignant lesion, without the need of tumor sensitizers and therefore with no additional complications to standard bronchoscopy techniques. The detection rate of high-grade dysplasia and carcinoma in-situ (CIS) is increased to 88% after using AFB, up from the median 40% detection rate that conventional white-light bronchoscopy provides [161, 162]. However, as already stated, both premalignant lesions and various inflammatory conditions have similar appearances in AFB. Therefore, the specificity is rather low, with a high rate of false positive investigations [163, 164].

Since diffuse reflectance spectroscopy measures directly the changes in the path of white light through tissue scattering and absorption levels, some have theorized that combining autofluorescence with diffuse reflectance probes may enhance the specificity of this method. Preliminary findings have shown that a combination between the two can significantly improve the positive predictive value of AFB without altering the already attained high sensitivity for premalignant and early malignant lesions [165] (Bard MPL et al, 2005). Other attempts to improve specificity by local spectroscopical measurements have shown promising results, making way for one-stop techniques which would combine two types of wavelength measurement and fluorophore weighting [153, 165].

One study investigated the use of AFB in primary lung cancer, after treatment of head and neck cancer, detecting 29% (12/44 patients) of all second primary lung cancers, while detecting early lesions in two patients which would otherwise be missed by conventional imaging

methods [166]. Early reports of Lam and his team in asbestos and diesel-exposed individuals showed an 86% sensitivity for moderate to severe dysplasia and CIS in the case of AFB, compared to just 52% for white light bronchoscopy [167]. A multicenter study performed by Lam in 1998 with the LIFE system, on 173 patients (142 biopsy-proven cases of severe dysplasia, CIS or invasive cancer) showed that AFB has a relative sensitivity of 2.71 compared to conventional bronchoscopy, successfully detecting 91 cases in comparison to only 35 with bronchoscopy alone. When considering intraepithelial lesions alone, the relative sensitivity increases to 6.1 for AFB compared to standard bronchoscopy [164].

A correlation between the loss of fluorescence and the grade of dysplasia; therefore, a trained endoscopist can differentiate these gradations to some extent, being even able to identify inflammatory or granulomatous lesions [155]. This would In turn greatly improve the specificity of AFB. A different approach consists in the usage of computer assisted analysis of signals of different wavelengths, represented in a spectrogram which in turn can classify benign from malignant lesions.

4. Narrow-Band Imaging (NBI)

NBI is a novel imaging technique capable of improving the visualization of superficial structures of the respiratory mucosa [168, 169]. NBI is used for an accurate classification of lesions, even though it does not have an established role during routine bronchoscopy [170–172]. High magnification bronchoscopy in combination with NBI can visualize the altered micro-vascularization which is formed in dysplastic or neoplastic lesions [173]. As the tumor progresses, it requires an adequately enlarged blood supply, therefore in most cancers, including those of the lungs and airways, neo angiogenesis is a constant phenomenon through which newly formed vessels are constantly produced in order to supplement local needs. These vessels form irregular aberrant patterns, having unequal diameters, tortuous configurations and uneven segment lengths.

The principle of NBI is simple: three optical filters segment the RGB (red-green-blue) light spectrum in sequence, thus narrowing the bandwidth of the spectral transmittance [174]. This allows for visual marking of capillary structures of the sub-mucosa in deep red color, allowing an easier identification and characterization, as different wavelengths penetrate the tissue at different depths. The filtering system is placed in the optical illumination system and basically contains two narrow wavelength components: NBI-B corresponding to the 400-430 nm range (blue and green visualization) and NBI-G for the 530-550 nm range (red visualization), while a third filter can be installed for an accurate segmentation of the blue-green features, operating in the 430-460 nm range; the optical light-source usually operates in the 400-700 nm wavelength range. All current models include a 2-filter system, which emphasizes capillaries in the superficial mucosal layers by the 400-430 nm light, coloring them in shades of brown, while deeper mucosal or submucosal vessels are displayed in cyan by using the 530-550 nm filter. Modern systems allow for easy switch between the normal WLI and the enhanced NBI operations [168].

Limitations of the technology arise from the fact that not all lung malignancies develop submucosal neo vascularization visible from the airways, therefore potential false-negative NBI findings can be frequent when used in combination with WLB. Its sensitivity may be however increased when used in conjunction with other specific techniques such as AFB; however, its role in the screening process for lung malignancies is yet to be determined. A step further in this direction would be the standardization of imaging findings, based on clinical descriptions and classification of abnormal airway vascularity. High magnification bronchoscopy can improve the specificity of the technique, as it may allow a more clear description of the vascular patterns [168]. Good prospects come from new techniques such as probe-based confocal laser endomicroscopy which can provide an in situ diagnosis of malignancy if used in conjunction with any endoscopic technique.

5. Probe-based Confocal Laser Endomicroscopy (pCLE)

Gastrointestinal applications of pCLE are numerous, the system being successfully tested in real-life conditions [175]. It can be used for identifying premalignant lesions otherwise invisible to classic endoscopic techniques, such as Barrett's esophagus [176], classification of polipous lesions at colonic level [177], gastric metaplasia or early stage lesions at all levels of the digestive tracts [178, 179]. The technique requires injection of fluorescein or another fluorophore, followed by endoscopic imaging of the dye to identify mucosal details such as mucosal and vessel architecture to distinguish among normal, dysplastic, and neoplastic tissue. The use of fluorescein as an in-vivo contrast agent for detecting vascular structures has been deemed safe by several studies [180]. It thus allows for better visualization of vascular structures, serving as an overall tissue contrasting agent as it may leak beyond capillary confinement.

The imaging microprobe is connected to 30,000 fiber-optic threads that enable point-to-point real-time detection at 12 frames/sec. The microprobe's flexibility and size (1.5 mm in diameter) allow for great user maneuverability to scan tissues in situ at angles that would not be possible with any available confocal microscope objective. The mini-probe is inserted through a working channel of any standard bronchoscope and can reach the alveolar duct. A laser generator emits 488 nm blue argon laser light which is transmitted through the optical fibers and excites the elastin scaffold of the acinus. In turn, a real time image of the elastic fibers which sustain the alveoli, as well as the microvessel architecture is revealed. The probe can be translated over a larger tissue sample, and the images later reconstructed in order to extend the field of view covered [181]. A monitor attached to an imaging unit is available for real-time visualization of cellular images, the device being capable of recording full length movies which can be recorded and later on analyzed with dedicated software [182].

This technology is still in its early stages; however, it was deemed safe by regulatory organisms in the United States of America for applications in patient settings. In conjunction with safe contrasting agents such as fluorescein [183] or methilen blue [184], it can be used for the

in vivo histologic assessment of the bronchial epithelium at all levels of the airway system [185–187]. Several studies reported good initial results in control groups of healthy smokers or patients with chronic obstructive pulmonary disease for diagnosing various forms of parenchymal lung disease [188, 189]. A pCLE investigation seems to be a quick and safe procedure for patients with various pulmonary conditions, with minimal side-effects related to both the technique and the contrasting fluorescent agents used for imaging. General consensus is that further studies are needed in order to extent the diagnostic capabilities and enhance its sensibility in comparison with standard cytological and histological techniques.

Author details

Mihai Olteanu[1], Costin Teodor Streba[1], Bogdan Oprea[1], Raluca Marinas[1], Mimi Floarea Nitu[1], Emilia Crisan[1,2] and Tudorel Ciurea[1]

1 University of Medicine and Pharmacy of Craiova, Romania

2 "Marius Nasta" Pulmonology Institute, Bucharest, Romania

References

[1] Lopez-Encuentra A, Garcia-Lujan R, Rivas JJ, Rodriguez-Rodriguez J, Torres-Lanza J, Varela- Simo G. Comparison between clinical and pathologic staging in 2,994 cases of lung cancer. Ann Thorac Surg 2005; 79:974–979; discussion, 979.

[2] Mountain CF. Revisions in the international system for staging lung cancer. Chest 1997; 111 (6): 1710-1717.

[3] Lung. In: American Joint Committee on Cancer. AJCC Cancer Staging Manual. 6th ed. New York, NY: Springer, 2002, pp 167-181.

[4] Silvestri GA. A seismic shift in staging. J Thorac Oncol 2007; 2 (8): 682-683.

[5] Goldstraw P Crowley JJ; on behalf of the IASLC International Staging Project. The International Association for the Study of Lung Cancer International Staging Project on Lung Cancer. J Thorac Oncol 2006; 1 (4): 281-286.

[6] Rami Porta R. Nueva clasificación TNM del cáncer de pulmón. Arch Bronconeumol 2009; 45 (4): 159-161.

[7] Sobin LH, Gospodarowicz MK, Wittekind C. eds. TNM Classification of Malignant Tumours, 7th ed., 2010, Wiley-Blackwell.

[8] Rami-Porta R, Crowley JJ, Goldstraw P. The revised TNM staging system for lung cancer. Ann Thorac Cardiovasc Surg 2009; 15 (1): 4-9.

[9] Groome PA, Bolejack V, Crowley JJ, Kennedy C, Krasnik M, Sobin LH, Goldstraw P; IASLC International Staging Committee; Cancer Research and Biostatistics; Observers to the Committee; Participating Institutions. The IASLC Lung Cancer Staging Project: validation of the proposals for revision of the T, N, and M descriptors and consequent stage groupings in the forthcoming (seventh) edition of the TNM classification of malignant tumours. J Thorac Oncol 2007; 2 (8): 694-705.

[10] Krasnik M, Vilmann P, Larsen S, Jacobsen G, Preliminary experience with a new method of endoscopic transbronchial real time ultrasound guided biopsy for diagnosis of mediastinal and hilar lesions Thorax. 2003 December; 58(12): 1083–1086.

[11] Herth F J F, Eberhardt R, Vilmann P, Krasnik M, Ernst A, Real-time endobronchial ultrasound guided transbronchial needle aspiration for sampling mediastinal lymph nodes, Thorax. 2006 September; 61(9): 795–798.

[12] Herth FJF, Krasnik M, Yasufuku K, R Rintoul R, Ernst A, Endobronchial Ultrasound-guided Transbronchial Needle Aspiration, J Bronchol 2006;13:84–91

[13] Wong M, Yasufuku K, Nakajima T, Herth FJ, Sekine Y, Shibuya K, Iizasa T, Hiroshima K, Lam WK, Fujisawa T, Endobronchial ultrasound: new insight for the diagnosis of sarcoidosis, Eur Respir J. 2007 Jun; 29(6):1182-6.

[14] Herth FJF, Ernst A, Eberhardt R, Vilmann P, Dienemann H, Krasnik M, Endobronchial Ultrasound-guided Transbronchial Needle Aspiration of Lymph Nodes in the Radiologically Normal Mediastinum. Eur Respir J 2006; 28: 910-914.

[15] Hwangbo B, Kim SK, Lee HS, Lee HS, Kim MS, Lee JM, Kim HY, Lee GK, Nam BH, Zo JI, Application of endobronchial ultrasound-guided transbronchial needle aspiration following integrated PET/CT in mediastinal staging of potentially operable non-small cell lung cancer. Chest. 2009 May;135(5):1280-7. Epub 2008 Dec 31.

[16] Ernst A, Anantham D, Eberhardt R, Krasnik M, Herth FJ. Diagnosis of mediastinal adenopathy-real-time endobronchial ultrasound guided needle aspiration versus mediastinoscopy. J Thorac Oncol. 2008 Jun;3(6):577-82.

[17] Herth FJ, Yasufuku K, Eberhardt R, Hoffmann H, Krasnik M, Ernst A. Resistance index in mediastinal lymph nodes: a feasibility study. J Thorac Oncol. 2008 Apr;3(4): 348-50.

[18] Herth F, Eberhardt R, Mulay T, Anantham D, Ernst A, Resistance index through EBUS in enlarged mediastinal lymph nodes correlates with malignant involvement, CHEST. October 2007;132(4_MeetingAbstracts):465c-466.

[19] Nakajima T, Yasufuku K, Suzuki M, et al. Assessment of epidermal growth factor receptor mutation by endobronchial ultrasound-guided transbronchial needle aspiration CHEST 2007;132(2):597-602.

[20] Nakajima T, Yasufuku K, Suzuki M, et al. Chemosensitivity-related aberrant methylation profiling of non-small cell lung cancer by endobronchial ultrasound-guided transbronchial needle aspiration CHEST 2007;132(4_MeetingAbstracts):466a-466.

[21] Tournoy KG, Annema JT, Krasnik M, Herth FJ, van Meerbeeck JP Endoscopic and endobronchial ultrasonography according to the proposed lymph node map definition in the seventh edition of the tumor, node, metastasis classification for lung cancer. J Thorac Oncol. 2009 Dec;4(12):1576-84.

[22] Annema JT, van Meerbeeck JP, Rintoul RC, Dooms C, Deschepper E, Dekkers OM, De Leyn P, Braun J, Carroll NR, Praet M, de Ryck F, Vansteenkiste J, Vermassen F, Versteegh MI, Veseliç M, Nicholson AG, Rabe KF, Tournoy KG. Mediastinoscopy vs endosonography for mediastinal nodal staging of lung cancer: a randomized trial. JAMA. 2010 Nov 24;304(20):2245-52.

[23] Hwangbo B, Lee G, Lee H, et al. Transbronchial and transesophageal fine-needle aspiration using an ultrasound bronchoscope in mediastinal staging of potentially operable lung cancer CHEST 2010;138(4):795-802, Herth FF, Krasnik M, Kahn N, Eberhardt R, Ernst A. Combined endoscopic-endobronchial ultrasound-guided fine-needle aspiration of mediastinal lymph nodes through a single bronchoscope in 150 patients with suspected lung cancer CHEST 2010;138(4):790-794.

[24] Herth FJ Nonsurgical staging of the mediastinum: EBUS and EUS. Semin Respir Crit Care Med. 2011 Feb;32(1):62-8. Epub 2011 Apr 15

[25] Edge SB, Byrd DR, Compton CC, Fritz AG, Greene FL, Trotti A. eds. Part I. General information on cancer staging and end-results reporting. 1. Purposes and principles of cancer staging. In: Edge SB, Byrd DR, Compton CC, Fritz AG, Greene FL, Trotti A. eds. AJCC Cancer Staging Manual. 7th ed., 2010, Springer; pp. 3-14.

[26] Herth FJ, Eberhardt R, Vilmann P et al. Real-time endobronchial ultrasound guided transbronchial needle aspiration for sampling mediastinal lymph nodes. Thorax 2006; 61: 795–798.

[27] Ernst A, Eberhardt R, Krasnik M, Herth FJ. Efficacy of endobronchial ultrasoundguided transbronchial needle aspiration of hilar lymph nodes for diagnosing and staging cancer. J Thorac Oncol 2009; 4: 947–950.

[28] Tournoy KG, Rintoul RC, van Meerbeeck JP et al. EBUS-TBNA for the diagnosis of central parenchymal lung lesions not visible at routine bronchoscopy. Lung Cancer 2009; 63: 45–49.

[29] Ernst A, Anantham D, Eberhardt R et al. Diagnosis of mediastinal adenopathy real-time endobronchial ultrasound guided needle aspiration versus mediastinoscopy. J Thorac Oncol 2008; 3: 577–582.

[30] Detterbeck FC, Jantz MA, Wallace MB et al. Invasive mediastinal staging of lung cancer. ACCP evidence based clinical practice guidelines, 2nd edition. Chest 2007; 132: 202S–220S..

[31] Tournoy KG, Govaerts E, Malfait T, Dooms C. Endobronchial ultrasound-guided transbronchial needle biopsy for M1 staging of extrathoracic malignancies. Ann Oncol first published online July 5, 2010 doi:10.1093/annonc/mdq311

[32] American Cancer Society. Cancer facts and figures, 1998. Atlanta, GA: American Cancer Society, 1998.

[33] A. Ernst, F.J.F. Herth (eds.), Endobronchial Ultrasound, DOI 10.1007/978-0-387-09437-3_1, ª Springer ScienceþBusiness Media, LLC 2009

[34] Silvestri GA, Gould MK, Margolis ML, et al. Noninvasive staging in non-small cell lung cancer: ACCP evidenced-based clinical practice guidelines (2nd edition). Chest. 2007; 132: 178–201

[35] Bhutani MS, Hawes RH, Hoffmann BJ. A comparison of the accuracy of echo features during endoscopic ultrasound (EUS) and EUS-guided fine-needle aspiration for diagnosis of malignant lymph node invasion. Gastrointest Endosc. 1997; 31: 550–553.

[36] Okamoto H, Watanabe K, Nagatomo A, et al. Endobronchial ultrasonography for mediastinal and hilar lymph node metastases of lung cancer. Chest. 2002; 121: 1498–1506.

[37] Yasufuku node staging in non-small cell carcinoma. Do we have to accept the compromise? Eur J Cardiothorac Surg. 2001; 20: 652–654.

[38] Rami-Porta R, Ball D, Crowley J, Giroux DJ, Jett J, Travis WD, Tsuboi M, Vallières E, Goldstraw P; International Staging Committee; Cancer Research and Biostatistics; Observers to the Committee; Participating Institutions. The IASLC Lung Cancer Staging Project: proposals for the revision of the T descriptors in the forthcoming (seventh) edition of the TNM classification for lung cancer. J Thorac Oncol 2007; 2 (7): 593-602.

[39] Postmus PE, Brambilla E, Chansky K, Crowley J, Goldstraw P, Patz EF Jr, Yokomise H; International Association for the Study of Lung Cancer International Staging Committee; Cancer Research and Biostatistics; Observers to the Committee; Participating Institutions. The IASLC Lung Cancer Staging Project: proposals for revision of the M descriptors in the forthcoming (seventh) edition of the TNM classification of lung cancer. J Thorac Oncol 2007; 2 (8): 686-693.

[40] Dr. A. De la Guerra. New TNM Classification for Lung Cancer. Part II: A review. Doctors Lounge Website. Available at: http://www.doctorslounge.com/index.php/articles/page/342.

[41] Strand TE, Rostad H, Møller B, Norstein J. Survival after resection for primary lung cancer: a population based study of 3211 resected patients. Thorax 2006; 61 (8): 710-715.

[42] Suzuki K, Nagai K, Yoshida J, Nishimura M, Takahashi K, Yokose T, Nishiwaki Y. Conventional clinicopathologic prognostic factors in surgically resected nonsmall cell lung carcinoma. A comparison of prognostic factors for each pathologic TNM stage based on multivariate analyses. Cancer 1999; 86 (10): 1976-1984.

[43] van Rens MT, de la Rivière AB, Elbers HR, van Den Bosch JM. Prognostic assessment of 2,361 patients who underwent pulmonary resection for non-small cell lung cancer, stage I, II, and IIIA. Chest 2000; 117 (2): 374-379.

[44] Hung JJ, Hsu WH, Hsieh CC, Huang BS, Huang MH, Liu JS, Wu YC. Post-recurrence survival in completely resected stage I non-small cell lung cancer with local recurrence. Thorax 2009; 64 (3): 192-196.

[45] Casali C, Storelli E, Morandi U. The prognostic impact of tumor size in resected stage I non-small cell lung cancer: evidence for a two thresholds tumor diameters classification. Lung Cancer 2006; 54 (2): 185-191.

[46] Mountain CF, Carr DT, Anderson WA. A system for the clinical staging of lung cancer. Am J Roentgenol Radium Ther Nucl Med 1974; 120 (1): 130-138.

[47] Ruffini E, Filosso PL, Bruna MC, Coni F, Cristofori RC, Mossetti C, Solidoro P, Oliaro A. Recommended changes for T and N descriptors proposed by the International Association for the Study of Lung Cancer - Lung Cancer Staging Project: a validation study from a single-centre experience. Eur J Cardiothorac Surg 2009; 36 (6): 1037-1044.

[48] Fukui T, Mori S, Hatooka S, Shinoda M, Mitsudomi T. Prognostic evaluation based on a new TNM staging system proposed by the International Association for the Study of Lung Cancer for resected non-small cell lung cancers. J Thorac Cardiovasc Surg 2008; 136 (5): 1343-1348.

[49] Kassis ES, Vaporciyan AA, Swisher SG, Correa AM, Bekele BN, Erasmus JJ, Hofstetter WL, Komaki R, Mehran RJ, Moran CA, Pisters KM, Rice DC, Walsh GL, Roth JA. Application of the revised lung cancer staging system (IASLC Staging Project) to a cancer center population. J Thorac Cardiovasc Surg 2009; 138 (2): 412-418.

[50] Li Z, Yu Y, Lu J, Luo Q, Wu C, Liao M, Zheng Y, Ai X, Gu L, Lu S. Analysis of the T descriptors and other prognosis factors in pathologic stage I non-small cell lung cancer in China. J Thorac Oncol 2009; 4 (6): 702-709.

[51] Kameyama K, Takahashi M, Ohata K, Igai H, Yamashina A, Matsuoka T, Nakagawa T, Okumura N. Evaluation of the new TNM staging system proposed by the International Association for the Study of Lung Cancer at a single institution. J Thorac Cardiovasc Surg 2009; 137 (5): 1180-1184.

[52] Mountain CF. Revisions in the international system for staging lung cancer. Chest 1997; 111 (6): 1710-1717.

[53] Naruke T, Tsuchiya R, Kondo H, Asamura H. Prognosis and survival after resection for bronchogenic carcinoma based on the 1997 TNM staging classification: the Japanese experience. Ann Thorac Surg 2001; 71(6): 1759-1764.

[54] Warren S, Gates O. Multiple primary malignant tumors: a survey of the literature and a statistical study. Am J Cancer 1932; 16: 1358-1414.

[55] Howe HL (ed). A review of the definition for multiple primary cancers in the United States. Workshop proceedings from December 4-6, 2002, in Princeton, New Jersey. Springfield (IL): North American Association of Central Cancer Registries, May 2003.

[56] Martini N, Melamed MR. Multiple primary lung cancers. J Thorac Cardiovasc Surg 1975; 70 (4): 606-612.

[57] Facility Oncology Registry Data Standards (FORDS): Revised for 2009. Chicago, Illinois: Commission on Cancer, American College of Surgeons; 2002.

[58] Johnson CH, Adamo M (eds.), SEER Program Coding and Staging Manual 2007. National Cancer Institute, NIH Publication number 07-5581, Bethesda, MD 2008 revision. Appendix C - Site-Specific Coding Modules. Part 3 C30.0 -C39.9: pgs 375-526.

[59] Shen KR, Meyers BF, Larner JM, Jones DR; American College of Chest Physicians. Special treatment issues in lung cancer: ACCP evidence-based clinical practice guidelines (2nd edition). Chest 2007; 132 (3 Suppl): 290S-305S.

[60] Deslauriers J, Brisson J, Cartier R, Fournier M, Gagnon D, Piraux M, Beaulieu M. Carcinoma of the lung. Evaluation of satellite nodules as a factor influencing prognosis after resection. J Thorac Cardiovasc Surg 1989; 97 (4): 504-512.

[61] Martini N, Melamed MR. Multiple primary lung cancers. J Thorac Cardiovasc Surg 1975; 70 (4): 606-612.

[62] Shen KR, Meyers BF, Larner JM, Jones DR; American College of Chest Physicians. Special treatment issues in lung cancer: ACCP evidence-based clinical practice guidelines (2nd edition). Chest 2007; 132 (3 Suppl): 290S-305S.

[63] Urschel JD, Urschel DM, Anderson TM, Antkowiak JG, Takita H. Prognostic implications of pulmonary satellite nodules: are the 1997 staging revisions appropriate? Lung Cancer 1998; 21 (2): 83-87.

[64] Rao J, Sayeed RA, Tomaszek S, Fischer S, Keshavjee S, Darling GE. Prognostic factors in resected satellite-nodule T4 non-small cell lung cancer. Ann Thorac Surg 2007; 84 (3): 934-938.

[65] Goldstraw P, Crowley J, Chansky K, Giroux DJ, Groome PA, Rami-Porta R, Postmus PE, Rusch V, Sobin L; International Association for the Study of Lung Cancer International Staging Committee; Participating Institutions. The IASLC Lung Cancer Stag-

ing Project: proposals for the revision of the TNM stage groupings in the forthcoming (seventh) edition of the TNM Classification of malignant tumours. J Thorac Oncol 2007; 2 (8): 706-714.

[66] Molina JR. The case of a good satellite: outcomes of resected ipsilateral same-lobe satellite pulmonary nodules. Chest 2009; 136 (3): 660-662.

[67] Pennathur A, Lindeman B, Ferson P, Ninan M, Quershi I, Gooding WE, Schuchert M, Christie NA, Landreneau RJ, Luketich JD. Surgical resection is justified in non-small cell lung cancer patients with node negative T4 satellite lesions. Ann Thorac Surg 2009; 87 (3): 893-899.

[68] Sobin LH, Wittekind C eds. Lung and pleural tumours. In: Sobin LH, Wittekind C eds. UICC International Union Against Cancer, TNM classification of malignant tumours, 6th ed. New York: Wiley-Liss, 2002; pp. 97-107.Even so, some authors use the term as a synonym for pleural nodules.

[69] Sobin LH, Wittekind C eds. Lung and pleural tumours. In: Sobin LH, Wittekind C eds. UICC International Union Against Cancer, TNM classification of malignant tumours, 6th ed. New York: Wiley-Liss, 2002; pp. 97-107.Even so, some authors use the term as a synonym for pleural nodules.

[70] Hammar SP. Common tumors. In: Dail DH, Hammar SP, eds. Pulmonary pathology, 2nd ed. New York: Springer-Verlag, 1994; pp. 1123–1278.

[71] Travis WD, Brambilla E, Rami-Porta R, Vallières E, Tsuboi M, Rusch V, Goldstraw P; International Staging Committee. Visceral pleural invasion: pathologic criteria and use of elastic stains: proposal for the 7th edition of the TNM classification for lung cancer. J Thorac Oncol 2008; 3 (12): 1384-1390.

[72] Mountain CF. Revisions in the international system for staging lung cancer. Chest 1997; 111 (6): 1710-1717.

[73] Antony VB, Loddenkemper R, Astoul P, Boutin C, Goldstraw P, Hott J, Rodriguez Panadero F, Sahn SA. Management of malignant pleural effusions. Eur Respir J 2001; 18 (2): 402-419.

[74] American Thoracic Society. Management of malignant pleural effusions. Am J Respir Crit Care Med 2000; 162 (5): 1987-2001.

[75] Antunes G, Neville E, Duffy J, Ali N; Pleural Diseases Group, Standards of Care Committee, British Thoracic Society. BTS guidelines for the management of malignant pleural effusions. Thorax 2003; 58 (Suppl 2): ii29-ii38.

[76] Sahn SA. Pleural diseases related to metastatic malignancies. Eur Respir J 1997; 10 (8): 1907-1913.

[77] Heffner JE, Nietert PJ, Barbieri C. Pleural fluid pH as a predictor of survival for patients with malignant pleural effusions. Chest 2000; 117 (1): 79-86.

[78] Osaki T, Sugio K, Hanagiri T, Takenoyama M, Yamashita T, Sugaya M, Yasuda M, Yasumoto K. Survival and prognostic factors of surgically resected T4 non-small cell lung cancer. Ann Thorac Surg 2003; 75 (6): 1745-1751.

[79] Sugiura S, Ando Y, Minami H, Ando M, Sakai S, Shimokata K. Prognostic value of pleural effusion in patients with non-small cell lung cancer. Clin Cancer Res 1997; 3 (1): 47-50.

[80] Mott FE, Sharma N, Ashley P. Malignant pleural effusion in non-small cell lung cancer--time for a stage revision? Chest 2001; 119 (1): 317-318.

[81] Kameyama K, Huang CL, Liu D, Okamoto T, Hayashi E, Yamamoto Y, Yokomise H. Problems related to TNM staging: patients with stage III non-small cell lung cancer. J Thorac Cardiovasc Surg 2002; 124 (3): 503-510.

[82] Sawabata N, Matsumura A, Motohiro A, Osaka Y, Gennga K, Fukai S, Mori T; Japanese National Chest Hospital Study group for Lung Cancer. Malignant minor pleural effusion detected on thoracotomy for patients with non-small cell lung cancer: is tumor resection beneficial for prognosis? Ann Thorac Surg 2002; 73 (2): 412-415.

[83] Osaki T, Sugio K, Hanagiri T, Takenoyama M, Yamashita T, Sugaya M, Yasuda M, Yasumoto K. Survival and prognostic factors of surgically resected T4 non-small cell lung cancer. Ann Thorac Surg 2003; 75 (6): 1745-1751.

[84] Rodriguez Panadero F. Lung cancer and ipsilateral pleural effusion. Ann Oncol 1995; 6 (Suppl 3): S25-S27.

[85] Ohta Y, Tanaka Y, Hara T, Oda M, Watanabe S, Shimizu J, Watanabe Y. Clinicopathological and biological assessment of lung cancers with pleural dissemination. Ann Thorac Surg 2000; 69 (4): 1025-1029.

[86] Sugiura S, Ando Y, Minami H, Ando M, Sakai S, Shimokata K. Prognostic value of pleural effusion in patients with non-small cell lung cancer. Clin Cancer Res 1997; 3 (1): 47-50.

[87] Maruyama R, Yokoyama H, Seto T, Nagashima S, Kashiwabara K, Araki J, Semba H, Ichinose Y. Catheter drainage followed by the instillation of bleomycin to manage malignant pericardial effusion in non-small cell lung cancer: a multi-institutional phase II trial. J Thorac Oncol 2007; 2 (1): 65-68.

[88] Kunitoh H, Tamura T, Shibata T, Imai M, Nishiwaki Y, Nishio M, Yokoyama A, Watanabe K, Noda K, Saijo N; JCOG Lung Cancer Study Group, Tokyo, Japan. A randomised trial of intrapericardial bleomycin for malignant pericardial effusion with lung cancer (JCOG9811). Br J Cancer 2009; 100 (3): 464-469.

[89] Kaira K, Takise A, Kobayashi G, Utsugi M, Horie T, Mori T, Imai H, Inazawa M, Mori M. Management of malignant pericardial effusion with instillation of mitomycin C in non-small cell lung cancer. Jpn J Clin Oncol 2005; 35 (2): 57-60.

[90] Naruke T, Tsuchiya R, Kondo H, Asamura H, Nakayama H. Implications of staging in lung cancer. Chest 1997; 112 (4 Suppl): 242S-248S.

[91] Osaki T, Sugio K, Hanagiri T, Takenoyama M, Yamashita T, Sugaya M, Yasuda M, Yasumoto K. Survival and prognostic factors of surgically resected T4 non-small cell lung cancer. Ann Thorac Surg 2003; 75 (6): 1745-1751.

[92] Alon BN, Anson BL. Pleural effusion in patients with non-small cell carcinoma--stage IV and not T4. Lung Cancer 2007; 57 (1): 123.

[93] Mott FE, Sharma N, Ashley P. Malignant pleural effusion in non-small cell lung cancer-time for a stage revision? Chest 2001; 119 (1): 317-318.

[94] Kameyama K, Huang CL, Liu D, Okamoto T, Hayashi E, Yamamoto Y, Yokomise H. Problems related to TNM staging: patients with stage III non-small cell lung cancer. J Thorac Cardiovasc Surg 2002; 124 (3): 503-510.

[95] Leong SS, Rocha Lima CM, Sherman CA, Green MR. The 1997 International Staging System for non-small cell lung cancer: have all the issues been addressed? Chest 1999; 115 (1): 242-248.

[96] Naruke T, Tsuchiya R, Kondo H, Asamura H, Nakayama H. Implications of staging in lung cancer. Chest 1997; 112 (4 Suppl): 242S-248S.

[97] Rusch VW, Asamura H, Watanabe H, Giroux DJ, Rami-Porta R, Goldstraw P; Members of IASLC Staging Committee. The IASLC lung cancer staging project: a proposal for a new international lymph node map in the forthcoming seventh edition of the TNM classification for lung cancer. J Thorac Oncol 2009; 4 (5): 568-577.

[98] Rusch VW, Crowley J, Giroux DJ, Goldstraw P, Im JG, Tsuboi M, Tsuchiya R, Vansteenkiste J; International Staging Committee; Cancer Research and Biostatistics; Observers to the Committee; Participating Institutions. The IASLC Lung Cancer Staging Project: proposals for the revision of the N descriptors in the forthcoming seventh edition of the TNM classification for lung cancer. J Thorac Oncol 2007; 2 (7): 603-612.

[99] Rusch VW, Asamura H, Watanabe H, Giroux DJ, Rami-Porta R, Goldstraw, on Behalf of the Members of the IASLC Staging Committee. The IASLC lung cancer staging project: a proposal for a new international lymph node map in the forthcoming seventh edition of the TNM classification for lung cancer. J Thorac Oncol 2009;4:568-577.

[100] Rusch VW, Crowley J, Giroux DJ, Goldstraw P, Im JG, Tsuboi M, Tsuchiya R, Vansteenkiste J; International Staging Committee; Cancer Research and Biostatistics; Observers to the Committee; Participating Institutions. The IASLC Lung Cancer Staging Project: proposals for the revision of the N descriptors in the forthcoming seventh edition of the TNM classification for lung cancer. J Thorac Oncol 2007; 2 (7): 603-612.

[101] The International Association for the Study of Lung Cancer (IASLC) lymph node map, including the proposed grouping of lymph node stations into “zones” for the purposes of prognostic analyses. (Reprinted from Rusch VW, on Behalf of the Mem-

bers of the IASLC Staging Committee. The IASLC lung cancer staging project: a proposal for a new international lymph node map in the forthcoming seventh edition of the TNM classification for lung cancer. J Thorac Oncol. 2009;4:568-577.

[102] Lee JG, Lee CY, Bae MK, et al. Validity of International Association for the Study of Lung Cancer proposals for the revision of N descriptors in lung cancer. J Thorac Oncol2008; 3:1421 –1426.

[103] Annema JT, Rabe KF. EUS in non-small cell lung cancer. In RH Hawes, P Fockens (Eds.), Endosonography. Philadelphia: WB Saunders, 2006:61–72.

[104] Kramer H, van Putten JW, Douma WR, Smidt AA, van Dullemen HM, Groen HJ. Technical description of endoscopic ultrasonography with fine-needle aspiration for the staging of lung cancer. Respir Med 2005; 99:179-185.

[105] Navani N, Spiro SG, Janes SM, Mediastinal staging of NSCLC with endoscopic and endobronchial ultrasound, Nat Rev Clin Oncol. 2009 May; 6(5): 278–286. doi: 10.1038/nrclinonc.2009.39

[106] Murgu S, Colt H, University of California, Irvine, The EBUS Bronchoscopist: Exploring the mediastinum with endobronchial ultrasound, Module 1, 2011, available at http://www.bronchoscopy.org/education.

[107] van Overhagen H, Brakel K, Heijenbrok MW, et al. Metastases in supraclavicular lymph nodes in lung cancer: assessment with palpation, US, and CT. Radiology 2004;232:75– 80.

[108] Kumaran M, Benamore RE, Vaidhyanath R, et al. Ultrasound guided cytological aspiration of supraclavicular lymph nodes in patients with suspected lung cancer. Thorax 2005;60:229 –233.

[109] Sihoe AD, Lee TW, Ahuja AT, Yim AP. Should cervical ultrasonography be a routine staging investigation for lung cancer patients with impalpable cervical lymph nodes? Eur J Cardiothorac Surg 2004;25: 486–491.

[110] Prosch H, Strasser G, Sonka C, et al. Cervical ultrasound (US) and US-guided lymph node biopsy as a routine procedure for staging of lung cancer. Ultraschall Med 2007;28:598–603.

[111] Robin Smithuis Radiology department of the Rijnland Hospital in Leiderdorp, the Netherlands, available at http://www.radiologyassistant.nl/en/4646f1278c26f#.

[112] von Bartheld MB, Rabe KF, Annema JT. Transaortic EUS-guided FNA in the diagnosis of lung tumors and lymph nodes. Gastrointest Endosc 2009;69:345–349.

[113] Malay Sharma, Vishal Arya and CS RameshBabu (2011). Techniques of Linear Endobronchial Ultrasound, Ultrasound Imaging - Medical Applications, Igor V. Minin and Oleg V. Minin (Ed.), ISBN: 978-953-307-279-1, InTech, Available from: http://

www.intechopen.com/books/ultrasound-imaging-medical-applications/techniques-of-linear-endobronchial-ultrasound

[114] Dooms C, Vansteenkiste J, Van RD, De LP. Esophageal ultrasoundcontrolled fine needle aspiration for staging of mediastinal lymph nodes in patients with resectable lung cancer: do we always see the reality? J Thorac Oncol 2009;4:1043–1045.

[115] Hammar SP. Common tumors. In: Dail DH, Hammar SP, eds. Pulmonary pathology, 2nd ed. New York: Springer-Verlag, 1994; pp. 1123–1278.

[116] Shepherd FA, Crowley J, Van Houtte P, Postmus PE, Carney D, Chansky K, Shaikh Z, Goldstraw P; International Association for the Study of Lung Cancer International Staging Committee and Participating Institutions. The International Association for the Study of Lung Cancer lung cancer staging project: proposals regarding the clinical staging of small cell lung cancer in the forthcoming (seventh) edition of the tumor, node, metastasis classification for lung cancer. J Thorac Oncol 2007; 2 (12): 1067-1077.

[117] Vallières E, Shepherd FA, Crowley J, Van Houtte P, Postmus PE, Carney D, Chansky K, Shaikh Z, Goldstraw P; International Association for the Study of Lung Cancer International Staging Committee and Participating Institutions. The IASLC Lung Cancer Staging Project: proposals regarding the relevance of TNM in the pathologic staging of small cell lung cancer in the forthcoming (seventh) edition of the TNM classification for lung cancer. J Thorac Oncol 2009; 4 (9): 1049-1059.

[118] Travis WD, Giroux DJ, Chansky K, Crowley J, Asamura H, Brambilla E, Jett J, Kennedy C, Rami-Porta R, Rusch VW, Goldstraw P; International Staging Committee and Participating Institutions. The IASLC Lung Cancer Staging Project: proposals for the inclusion of broncho-pulmonary carcinoid tumors in the forthcoming (seventh) edition of the TNM Classification for Lung Cancer. J Thorac Oncol 2008; 3 (11): 1213-1223.

[119] Goldstraw P., editors. Staging manual in thoracic oncology. Orange Park, FL, USA: Rx Press; 2009.

[120] Dr. A. De la Guerra. New TNM Classification for Lung Cancer - Part I: The changes. Doctors Lounge Website. Available at: http://www.doctorslounge.com/index.php/articles/page/340.

[121] Detterbeck FC, Boffa DJ, Tanoue LT. The new lung cancer staging system. Chest 2009; 136 (1): 260-271.

[122] Torrington KC, Kern JD. The utility of fiberoptic bronchoscopy in the evaluation of the solitary pulmonary nodule. Chest 1993;104:1021–1024.

[123] Fletcher EC, Levin DC. Flexible fiberoptic bronchoscopy and fluoroscopically guided transbronchial biopsy in the management of solitary pulmonary nodules. West J Med 1982;136:477–483.

[124] Shure D, Fedullo PF. Transbronchial needle aspiration of peripheral masses. Am Rev Respir Dis 1983;128:1090–1092.

[125] Geraghty PR, Kee ST, McFarlane G, Razavi MK, Sze DY, Dake MD. CT-guided transthoracic needle aspiration biopsy of pulmonary nodules: needle size and pneumothorax rate. Radiology 2003;229:475–481.

[126] Kazerooni EA, Lim FT, Mikhail A, Martinez FJ. Risk of pneumothorax in CT-guided transthoracic needle aspiration biopsy of the lung. Radiology 1996;198:371–375.

[127] Ohno Y, Hatabu H, Takenaka D, et al. CT-guided transthoracic needle aspiration biopsy of small (, or520 mm) solitary pulmonary nodules. AJR Am J Roentgenol 2003;180:1665–1669.

[128] Kato R, Katada K, Anno H, Suzuki S, Ida Y, Koga S. Radiation dosimetry at CT fluoroscopy: physician's hand dose and development of needle holders. Radiology 1996;201:576–578.

[129] Baaklini W, Reinoso M, Gorin A, et al. Diagnostic yield of fiberoptic bronchoscopy in evaluating solitary pulmonary nodules. Chest 2000;117:1049-1054.

[130] Rajamani S, Mehta AC. Transbronchial needle aspiration of central and peripheral nodules. Monaldi Arch Chest Dis 2001;56:436–445.

[131] Horrow EM, Wajdy A, Blum J, Harkin T, Gasparini S, Addrizzo-Harris DJ, Arroliga AC, Wight G, Mehta A. The utility of transbronchial needle aspiration in the staging of bronchogenic carcinoma. Am J Respir Crit Care Med 2000;161:601–607.

[132] Daryl P. Pearlstein, MD, Society of Thoracic Surgeons in San Diego, Calif., February 2011.

[133] Markis D, Scherpereel A, Leroy S, et al. Electromagnetic navigation diagnostic bronchoscopy for small peripheral lung lesions. Eur Respir J 2007;29:1187-1192.

[134] Gildea TR, Mazzone PJ, Karnak D, Meziane M, Mehta AC. Electromagnetic navigation diagnostic bronchoscopy: a prospective study. Am J Respir Crit Care Med 2006;174:982–989.

[135] Goldberg SN, Raptopoulos V, Boiselle PM, Edinburgh KJ, Ernst A. Mediastinal lymphadenopathy: diagnostic yield of transbronchial mediastinal lymph node biopsy with CT fluoroscopic guidance-initial experience. Radiology 2000;216:764–767.

[136] Schenk DA, Chambers SL, Dardak S, Komadina KH, Pickard JS, Strollo PJ, Lewis RE, Patefield AJ, Henderson JH, Tomski SM. Comparison of Wang 19-gauge and 22-gauge needles in the mediastinal staging of lung cancer. Am Rev Respir Dis 1993;147:1251–1258.

[137] Wang KP, Britt EJ. Needle brush in the diagnosis of lung mass or nodule through flexible bronchoscopy. Chest 1991;100:1148–1150.

[138] Reichenberger F, Weber J, Tamm M, Bolliger CT, Dalquen P, Perruchoud AP, Soler M. The value of transbronchial needle aspiration in the diagnosis of peripheral pulmonary lesions. Chest 1999; 116:704–708.

[139] Eberhardt R, Anantham D, Herth F, Feller-Kopman D, Ernst A, Electromagnetic Navigation Diagnostic Bronchoscopy in Peripheral Lung Lesions, CHEST 2007;131:1800–1805.

[140] Becker HC, Herth F, Ernst A, et al. Bronchoscopic biopsy of peripheral lung lesions under electromagnetic guidance: a pilot study. J Bronchol 2005;12:9–13.

[141] Paone G, Nicastri E, Lucantoni G, et al. Endobronchial ultrasound-driven biopsy in the diagnosis of peripheral lung lesions. Chest 2005;128:3551–3557.

[142] Kikuchi E, Yamazaki K, Sukoh N, et al. Endobronchial ultrasonography with guide-sheath for peripheral pulmonary lesions. Eur Respir J 2004;24:533–537.

[143] Kurimoto N, Miyazawa T, Okimasa S, et al. Endobronchial ultrasonography using a guide sheath increases the ability to diagnose peripheral pulmonary lesions endoscopically. Chest 2004;126:959–965.

[144] Herth FJ, Ernst A, Becker HD. Endobronchial ultrasoundguided transbronchial lung biopsy in solitary pulmonary nodules and peripheral lesions. Eur Respir J 2002;20:972–974.

[145] Herth FJ, Eberhardt R, Becker HD, et al. Endobronchial ultrasound-guided transbronchial lung biopsy in fluoroscopically invisible solitary pulmonary nodules: a prospective trial. Chest 2006;129:147–150.

[146] Lechtzin N, Rubin HR, White P Jr, et al. Patient satisfaction with bronchoscopy. Am J Respir Crit Care Med 2002; 166:1326–1331.

[147] Suratt PM, Smiddy JF, Gruber B. Deaths and complications associated with fiberoptic bronchoscopy. Chest 1976;69:747–751.

[148] Sawabata N, Ohta M, Maeda H. Fine-needle aspiration cytologic technique for lung cancer has a high potential of malignant cell spread through the tract. Chest 2000;118:936–939.

[149] Gupta S, Krishnamurthy S, Broemeling LD, et al. Small (</=2-cm) subpleural pulmonary lesions: short- versus longneedle-path CT-guided biopsy; comparison of diagnostic yields and complications. Radiology 2005;234:631–637.

[150] DeCamp MM Jr, Jaklitsch MT, Mentzer SJ, et al. The safety and versatility of videothoracoscopy: a prospective analysis of 895 consecutive cases. J Am Coll Surg 1995;181:113–120.

[151] International Early Lung Cancer Action Program Investigators, Henschke CI, Yankelevitz DF, et al. Survival of patients with stage I lung cancer detected on CT screening. N Engl J Med 2006;355:1763–1771.

[152] Hirsch FR, Prindiville SA, Miller YE, et al. Fluorescence versus white-light bronchoscopy for detection of preneoplastic lesions: a randomized study. JNatl Cancer Inst 2001;93:1385—91.

[153] Hüttenberger D, Gabrecht T, Wagnières G et al. Autofluorescence detection of tumors in the human lung——Spectroscopical measurements in situ, in an in vivo model and in vitro. Photodiagnosis Photodyn Ther. 2008;5(2):139-47.

[154] Qu J, MacAulay S, Lam S, Palcic B. Laser-induced fluorescence spectroscopy at endoscopy: tissue optics, Monte-Carlo modeling and in vivo measurements. Optical Engineering 1995;34(11):3334—43.

[155] Nakhosteen JA, Khanavkar B. Autofluorescence Bronchoscopy: The Laser Imaging Fluorescence Endoscope. In: Interventional Bronchoscopy. Prog Respir Res. Bolliger CT, Mathur PN (eds). Basel, Karger, 2000, 30:236–242.

[156] Becker HD. Bronchoscopy and computer technology. In: Thoracic Endoscopy: Advances in Interventional Pulmonology. Simoff MJ, Sterman DH, Ernst A (Eds). Massachusetts, USA; Blackwell Publishing, 2006: 88–118.

[157] Morgan R, Ernst A. Advanced diagnostic bronchoscopy. In: Introduction to bronchoscopy. Ernst A (Ed). New York, USA. Cambridge University Press, 2009: 134–141.

[158] Herth FJ, Ernst A, Becker HD. Autofluorescence bronchoscopy—a comparison of two systems (LIFE and D-Light). Respiration 2003;70:395—8.

[159] Homasson JP, Capron F, Angebault M, Nguyen Bich N. Lung autofluorescence. Preliminary study of two systems without laser illumination or photosensitization. Review of Pneumological Clinics 2001;57:202—7.

[160] Goujon D, Zellweger M, Radu A, et al. In vivo autofluorescence imaging of early cancers in the human tracheobronchial tree with a spectrally optimized system. Journal of Biomedical Optics 2003;8:17—25.

[161] Kurie JM, Lee JS, Morice RC, et al. Autofluorescence bronchoscopy in the detection of squamous metaplasia and dysplasia in current and former smokers. J Natl Cancer Inst 1998;90:991—5.

[162] Wagnieres GA, Star WM, Wilson BC. In vivo fluorescence spectroscopy and imaging for oncological applications. Photochem Photobiol 1998;68:603—32.

[163] Lam S, MacAulay C, Hung J, et al. Detection of dysplasia and carcinoma in situ with a lung imaging fluorescence endoscope device. J Thorac Cardiovasc Surg 1993;105:1035–1040.

[164] Lam S, Kennedy T, Unger M, et al. Localization of bronchial intraepithelial neoplastic lesions by fluorescence bronchoscopy. Chest 1998;113:696–702.

[165] Bard MP, Amelink A, Skurichina M, den Bakker M et al. Improving the specificity of fluorescence bronchoscopy for the analysis of neoplastic lesions of the bronchial tree

by combination with optical spectroscopy: preliminary communication. Lung Cancer. 2005;47(1):41-7.

[166] Lee P, de Bree R, Brokx HA, et al. Primary lung cancer after treatment of head and neck cancer without lymph node metastasis: is there a role for autofluorescence bronchoscopy? Lung Cancer. 2008;62(3):309-15.

[167] Lam S, Hung J, Kennedy SM, et al: Detection of dysplasia and carcinoma in situ by ratio fluorometry. Am Rev Respir Dis 1992;146: 1458–1461.

[168] Yamada G, Kitamura Y, Kitada J et al. Increased microcirculation in subepithelial invasion of lung cancer. Intern Med. 2011;50:839-43.

[169] Vincent BD, Fraig M, SilvestriGA. Apilot study of narrow band imaging compared to white light bronchoscopy for evaluation of normal airways, pre-malignant and malignant airways disease. Chest. 2007;131(6):1794–1799.

[170] Kaltenbach T, Sano Y, Friedland S et al. American Gastroenterological Association (AGA) institute technology assessment on image-enhanced endoscopy. Gastroenterology 2008; 134: 327–40.

[171] Tajiri H, Niwa H. Proposal for a consensus terminology in endoscopy: how should different endoscopic imaging techniques be grouped and defined? Endoscopy 2008; 40: 775–8.

[172] Ohtani K, Lee AM, Lam S. Frontiers in bronchoscopic imaging. Respirology. 2012;17(2):261-9.

[173] Shibuya K, Hoshino H, Chiyo M, Iyoda A, Yoshida S, et al. High magnification bronchovideoscopy combined with narrow band imaging could detect capillary loops of angiogenic squamous dysplasia in heavy smokers at high risk for lung cancer. Thorax 2003;58:989-995.

[174] Gono K, Obi T, Yamaguchi M, Ohyama N, et al. Appearance of enhanced tissue features in narrow-band endoscopic imaging. J Biomed Opt. 2004;9(3):568-77.

[175] Liu H, Li YQ, Yu T, Zhao YA, Zhang JP, et al. Confocal endomicroscopy for in vivo detection of microvascular architecture in normal and malignant lesions of upper gastrointestinal tract. J Gastroenterol Hepatol 2008;23:56e61.

[176] Pohl H, Rosch T, Vieth M, Koch M, Becker V, et al. Miniprobe confocal laser microscopy for the detection of invisible neoplasia in patients with Barrett's oesophagus. Gut 2008;57: 1648e53.

[177] Buchner AM, Shahid MW, Heckman MG, Krishna M, Ghabril M, et al. Comparison of probe-based confocal laser endomicroscopy with virtual chromoendoscopy for classification of colon polyps. Gastroenterology 2009;138:834e42.

[178] Hoffman A, Goetz M, Vieth M, et al. Confocal laser endomicroscopy: technical status and current indications. Endoscopy. 2006;38:1275–1283.

[179] Hsiung PL, Hardy J, Friedland S, et al. Detection of colonic dysplasia in vivo using a targeted heptapeptide and confocal microendoscopy. Nat Med. 2008;14:454–458.

[180] Wallace MB, Meining A, Canto MI, Fockens P, Miehlke S, et al. The safety of intravenous fluorescein for confocal laser endomicroscopy in the gastrointestinal tract. Aliment Pharmacol Ther 2010;31:548e52.

[181] Thiberville L, Salaun M, Lachkar S, Dominique S, Moreno-Swirc S, et al. Human in vivo fluorescence microimaging of the alveolar ducts and sacs during bronchoscopy. Eur Respir J 2009;33:974e85.

[182] Newton RC, Kemp SV, Yang GZ et al. Imaging parenchymal lung diseases with confocal endomicroscopy. Respir Med. 2012;106(1):127-37.

[183] Fuchs FS, Zirlik S, Hildner K, Frieser M, Ganslmayer M, et al. Fluorescein-aided confocal laser endomicroscopy of the lung. Respiration 2011;81:32e8.

[184] Thiberville L, Salaun M, Lachkar S, Moreno-Swirc S, Bourg-Heckly G. In-vivo confocal endomicroscopy of peripheral lung nodules using 488nm/660nm induced fluorescence and topical methylene blue. Eur Respir Soc Berlin 2008:263se4s

[185] Thiberville L, Moreno-Swirc S, Vercauteren T, Peltier E, Cave C, et al. In vivo imaging of the bronchial wall microstructure using fibered confocal fluorescence microscopy. Am J Respir Crit Care Med 2007;175:22e31.

[186] Musani AI, Sims M, Sareli C, Russell W, McLaren WJ, et al. A pilot study of the feasibility of confocal endomicroscopy for examination of the human airway. J Bronchology Interv Pulmonology 2010;17:126e30.

[187] Lane PM, Lam S, McWilliams A, Leriche JC, Anderson MW, et al. Confocal fluorescence microendoscopy of bronchial epithelium. J Biomed Opt 2009;14:024008.

[188] Newton RC, Kemp S, Elson DS, Yang G-Z, Thomas CMR, et al. Confocal endomicroscopy in diffuse lung diseases – initial results and future directions. Am J Respir Crit Care Med 2010; 181:A6620.

[189] Newton RC, Kemp S, Yang GZ, Darzi A, Sheppard M, et al. Tracheobronchial amyloidosis and confocal endomicroscopy. Respiration 2011;82:209e11.

IntechOpen

IntechOpen